









Research Article

Avian skulls represent a diverse ornithuromorph fauna from the Lower Cretaceous Xiagou Formation, Gansu Province, China

Jingmai K. O'Connor^{1,2,3*} , Thomas A. Stidham^{2,3,4} , Jerald D. Harris⁵ , Matthew C. Lamanna⁶ , Alida M. Bailleul^{2,3} , Han Hu⁷ , Min Wang^{2,3} , and Hai-Lu You^{2,3,4} 

¹Negaunee Integrative Research Center, Field Museum of Natural History, Chicago, IL 60605, USA

²Key Laboratory of Vertebrate Evolution and Human Origins, Institute of Vertebrate Paleontology and Paleoanthropology, Chinese Academy of Sciences, Beijing 100044, China

³CAS Center for Excellence in Life and Paleoenvironment, Beijing 100044, China

⁴College of Earth and Planetary Sciences, University of Chinese Academy of Sciences, Beijing 100049, China

⁵Department of Earth and Environmental Sciences, Dixie State University, St. George, UT 84770, USA

⁶Section of Vertebrate Paleontology, Carnegie Museum of Natural History, Pittsburgh, PA 15213, USA

⁷Department of Earth Sciences, University of Oxford, Oxford, OX1 3AN, UK

*Author for correspondence. E-mail: jconnor@fieldmuseum.org

Received 2 September 2021; Accepted 9 December 2021; Article first published online 29 December 2021

Abstract We describe six specimens consisting of cranial remains and associated partial presacral axial series belonging to ornithuromorph birds from the Changma locality of the Lower Cretaceous Xiagou Formation of northwestern Gansu Province, China. Comparison among specimens is limited by the paucity of overlapping elements, their differing exposed views, and, in some specimens, poor preservation. Despite this, three separate taxa are represented, evidenced by differences in their dentary dentitions: one specimen is edentulous, another has sharp, closely spaced, relatively high-crowned and peg-like teeth, and a third preserves blunt, relatively low-crowned teeth placed in a communal groove, a morphology previously reported among adult birds only in Hesperornithiformes. We propose that the high-crowned specimen may be referred to *Gansus yumenensis* based on shared similarities with the closely related *Iteravis huchzermeyeri*, including a very similar dentition and an edentulous premaxilla with elongate, unfused frontal processes and no palatal processes. The two other specimens are considered new taxa, for which we erect the names *Meemannavis ductrix* gen. et sp. nov. and *Brevidentavis zhangii* gen. et sp. nov. These new specimens confirm that the Changma locality is dominated by ornithuromorph birds and contribute to a better understanding of this important avifauna. The observed variation in dental morphology hints at trophic diversity like that observed in ornithuromorphs from the penecontemporaneous Jehol Group of northeastern China.

Key words: Aves, avian cranium, Changma locality, Early Cretaceous, *Gansus*, Ornithuromorpha.

1 Introduction

The first Mesozoic bird described from Chinese deposits was *Gansus yumenensis* from the Lower Cretaceous (Aptian) Xiagou Formation of Gansu Province, northwestern China (Hou & Liu, 1984). The holotype of this ornithuromorph consists of an isolated left tarsometatarsus and pes. Approximately two decades later, renewed excavations in the Xiagou Formation exposed near the town of Changma in Gansu Province produced dozens of three-dimensionally preserved specimens referable to this taxon, ranging from fairly complete partial skeletons to isolated elements (Fig. 1). These new partial skeletons are typically articulated and sometimes preserve soft tissues. Based on these fossil specimens, the postcranial morphology of *G. yumenensis* has

been described thoroughly, with all parts except the most cranial cervical vertebrae known (Fig. 2A) (You et al., 2006; Li et al., 2011; Wang et al., 2016c).

In addition to *G. yumenensis*, four species of enantiornithine birds (*Avimaia schweitzerae* [Lamanna et al., 2006; Bailleul et al., 2019b], *Dunhuangia cuii* [Wang et al., 2015a], *Feitianius paradisi* [O'Connor et al., 2016b], and *Qiliania graffini* [Ji et al., 2011]), and three other species of ornithuromorphs (*Changmaornis houii*, *Jiuquanornis niui*, and *Yumenornis huangi* [Wang et al., 2013]), have been described from the Changma locality. Three enantiornithine specimens of indeterminate affinities also have been described (You et al., 2005; Harris et al., 2006; O'Connor et al., 2012). All specimens of these taxa consist of articulated but partial postcranial skeletons, with some preserving extensive soft

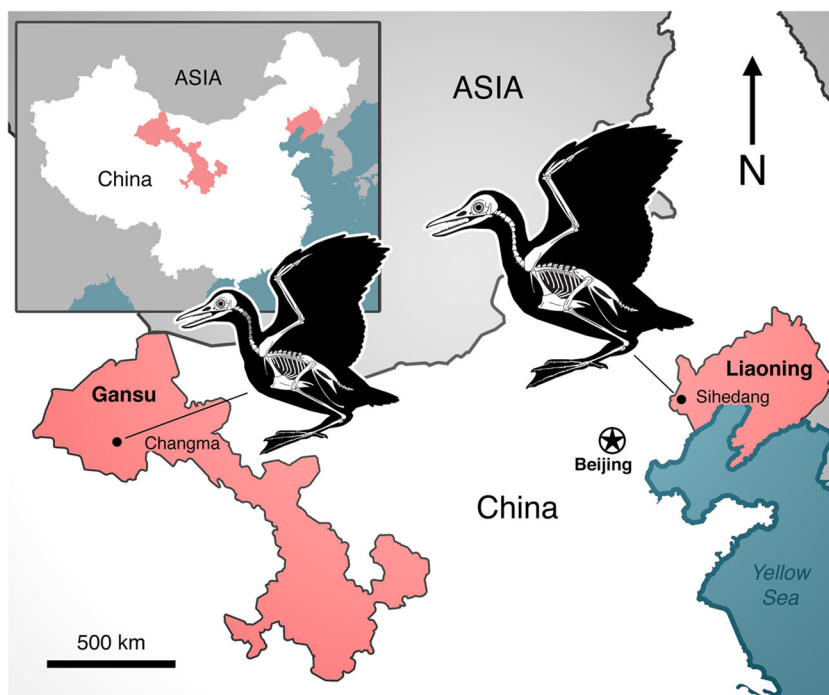


Fig. 1. Map of China indicating the positions of the Changma locality of the Xiagou Formation in Gansu Province, which has produced numerous specimens of the ornithuromorph *Gansus yumenensis* (pictured) and the six skull-bearing specimens described here, and the Sihedang locality of the Jehol Group in Liaoning Province, which has produced large numbers of the closely related *Iteravis huchzermeyeri* (pictured) (and its junior synonym or close relative *Ganus zheni*). Skeletal reconstructions based on reconstruction of *G. yumenensis* published by You et al. (2006; fig. 2k). Map modified from You et al. (2006; fig. 1) and Huang et al. (2016; fig. 1).

tissues (O'Connor et al., 2012, 2016b) and in one case, an unlaidd egg and rare medullary bone (Bailleul et al., 2019b). Avian skull material from the Changma locality has been mentioned previously, but only described cursorily (Harris et al., 2009). Birds are the most diverse part of the Xiagou Formation vertebrate fauna, which includes several species of fish (Ma, 1993; Murray et al., 2010), an undescribed salamander, and a species of turtle (represented by four specimens) (Brinkman et al., 2013). The Xiagou fauna recovered from the Changma locality thus is overwhelmingly dominated by birds in terms of the number of taxa and specimens, and this avifauna is, in turn, dominated by *G. yumenensis* (You et al., 2006; Li et al., 2011; Wang et al., 2015b). Almost all other paravian taxa are known from single specimens with the exception of the enantiornithines *Avimaia* and *Qiliania*, both known from two specimens (Lamanna et al., 2006; Ji et al., 2011; Bailleul et al., 2019b).

In 2013, the Sihedang locality in Liaoning Province (Fig. 1) was discovered within an exposure of strata belonging to the Jehol Group. Whether these strata pertain to the ~125 Ma Yixian Formation (Zhou et al., 2014; Lü & Brusatte, 2015; Hu & O'Connor, 2017; Wang et al., 2020a) or the ~120 Ma Jiufotang Formation (Liu et al., 2014; Lü et al., 2016b; Shao et al., 2018) is unclear from the available literature. However, recent stratigraphic analysis at Sihedang supports placement of this locality in the Jiufotang Formation (Yu & Meng, pers. comm.; Ju et al., 2021). Like Changma, this locality appears to be dominated by a single ornithuromorph taxon, in this case

Iteravis huchzermeyeri (Zhou et al., 2014) (Figs. 1, 2B), which is strikingly similar in its morphology to *G. yumenensis*, so much so that some specimens were assigned initially to a purported new species of the latter genus, *Gansus zheni* (Liu et al., 2014). Some authors regard *G. zheni* as a junior synonym of *I. huchzermeyeri* (Ju et al., 2021), which was described slightly earlier, a hypothesis supported by one phylogenetic analysis (Wang et al., 2018b). However, in light of minor observable differences of uncertain taxonomic significance, we choose to treat the two taxa separately here, pending a thorough study of all specimens referred to either *Iteravis* or *G. zheni*. Regardless, the close phylogenetic positions of *Iteravis* + *G. zheni* and *G. yumenensis* are consistent with the similarity of the Sihedang avifauna to that recovered from the Xiagou Formation at the Changma locality, which is inferred to be younger than the Yixian Formation and similar in age to the Jiufotang Formation (Suarez et al., 2013).

Most phylogenetic analyses resolve *Iteravis* (and *G. zheni*) as closely related to *G. yumenensis*, with *Iteravis* typically placed in a position just basal to the latter (Wang et al., 2018a, 2018b, 2019). At least one analysis resolves *Gansus* as monophyletic with *G. zheni* in an exclusive clade with *G. yumenensis* (Liu et al., 2014). Compared to most other Early Cretaceous ornithuromorphs, the pedal digits of *G. yumenensis* are elongate (digit III > tarsometatarsus) and gracile, a morphology that is also present in *Iteravis* (Zhou et al., 2014), *Yixianornis grabau*, and, to a lesser degree, *Yanornis martini* (which has somewhat more robust digits)

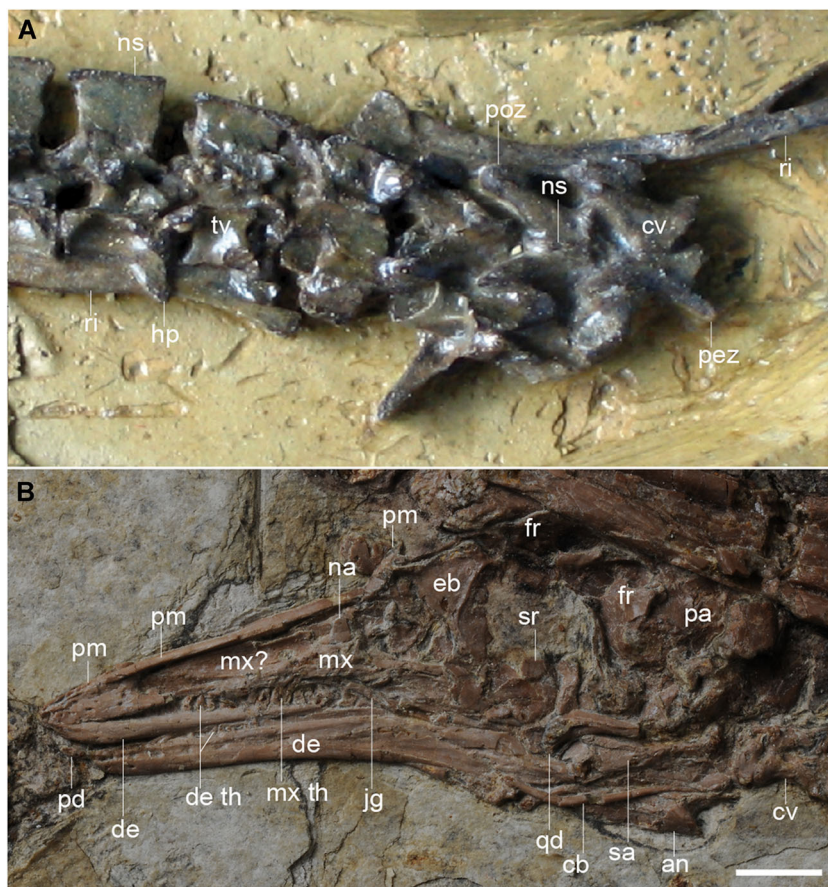


Fig. 2. A, Photograph of *Gansus yumenensis* (CAGS-IG-04-CM-002), preserving caudal cervical vertebrae (primarily in dorsal view) in articulation with cranial thoracic vertebrae (primarily in right lateral view). **B**, Photograph of skull of *Iteravis huchzermeyeri* (IVPP V18958) in left lateral view. Scale bar equals 5 mm.

(Zhou & Zhang, 2001) as well as hongshanornithids (in which digit III is approximately the same length as the tarsometatarsus) (Chiappe et al., 2014). The taxa that possess longer pedal digits likely occupied a different ecological niche than the Jehol ornithuromorphs that possess proportionally shorter and more robust tarsometatarsi and pedal digits (e.g., *Archaeorhynchus spathula*, *Bellulornis rectusunguis*, *Schizoura lii*) (Zhou et al., 2012, 2013; Wang et al., 2016b). Integument preserved with the feet of several specimens of *G. yumenensis* (e.g., IVPP V15074 and V15083, CAGS-IG-04-CM-008) has led some authors to suggest that the foot of this bird was webbed (Ji et al., 2006; You et al., 2006). Ecological analysis suggests this species may have engaged in shallow diving using its wings and/or hind limbs (Nudds et al., 2013).

Six avian specimens preserving skull material were collected from the Changma locality during field work in 2004 and 2005 (IVPP V26194, V26195, V26196, V26197, V26198, and V26199) (Figs. 3–8). In contrast to the largely three-dimensional postcranial-only specimens, the skulls are crushed or flattened and preserved primarily in two dimensions. Further obscuring the preserved morphologies, all six specimens have been coated with a layer of thick and highly reflective consolidant. All skull-bearing specimens appear referable to Ornithuromorpha based on a combination of their vertebral

morphology, fusion of the dentary with postdentary bones, the presence of a prementary bone in IVPP V26197 (Bailleul et al., 2019a), and the morphology of the premaxilla (rostrally fused and edentulous). Fused mandibular bones and edentulous, rostrally fused premaxillae are not found in Early Cretaceous enantiornithines, and, among birds, a prementary is found exclusively in non-neornithine ornithuromorphs (O'Connor & Chiappe, 2011; Bailleul et al., 2019a). However, given the absence of appendicular skeletal material preserved with the skulls, the specific taxonomic identification of these materials are problematic.

All skull specimens reported here also preserve associated cervical vertebrae. Three specimens even include a few poorly preserved cranial thoracic vertebrae (IVPP V26196, V26197, and V26198). Only two previously referred specimens of *G. yumenensis* preserve cervical vertebrae, and then only the most caudal elements (CAGS-IG-04-CM-002 and 04-CM-004) (You et al., 2006) (Fig. 2A). Thoracic vertebrae are present in several well-preserved specimens (CAGS-IG-04-CM-002, 04-CM-003 [mostly not exposed], and 04-CM-004; GSGM-07-CM-009 and 07-CM-011 [You et al., 2006; Wang et al., 2016c]). This means that the three new specimens that preserve only cranial (and, in two cases, middle) cervical vertebrae (IVPP V26194, V26195, and V26199) have no

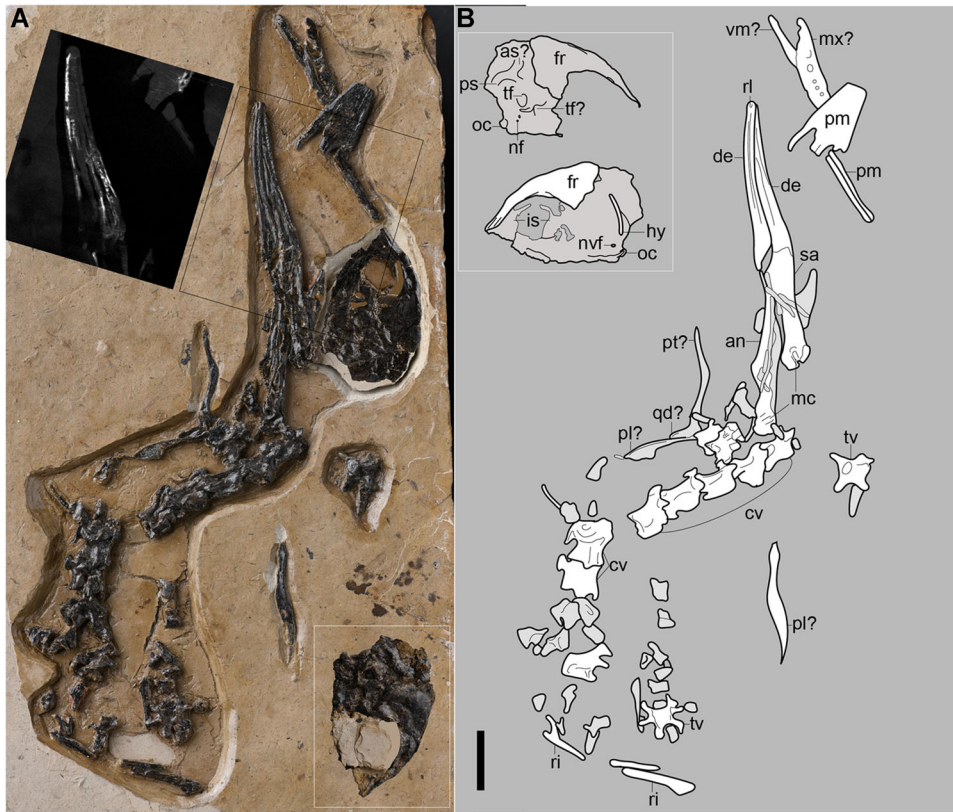


Fig. 3. Holotype of *Meemannavis ductrix* gen. et sp. nov. (IVPP V26198). **A**, Photograph. **B**, Interpretive drawings primarily in left lateral view. Scale bar equals 10 mm. In **A**, inset at upper left is computed tomographic image confirming absence of dentary teeth; inset at lower right is orbital region and braincase in right lateral view. In **B**, inset is orbital region and braincase in right (top) and left (bottom) lateral views.

osteological overlap with described *G. yumenensis* material. Even where overlap exists (i.e., the three specimens that preserve the most caudal cervical and cranial thoracic vertebrae: IVPP V26196, V26197, and V26198), differences in exposed surfaces or poor preservation of the vertebrae of the new specimens makes comparisons problematic.

The three other ornithuromorph taxa that have been described from the Xiagou Formation – *Changmaornis*, *Jiuquanornis*, and *Yumenornis* – are based on partial postcranial skeletons that preserve no overlapping elements with the six specimens described here (Wang et al., 2013). It is therefore impossible to determine if any of these new skull-bearing specimens are referable to these other Xiagou ornithuromorphs. Furthermore, these three named taxa may in fact represent only two distinct species. *Yumenornis* (known only from the partial sternum and furcula and right sternal ribs, pectoral girdle, and forelimb) and *Jiuquanornis* (known only from the sternum, sternal ribs, and furcula) can be differentiated from each other and from *G. yumenensis* based on the morphology of the sternum (You et al., 2010; Wang et al., 2013). In contrast, *Changmaornis* is known from only two thoracic vertebrae, a thoracic rib, the partial synsacrum and pelvic girdle, and the distal right hind limb, and therefore can be compared only to *G. yumenensis* (Wang et al., 2013). It is therefore conceivable that *Changmaornis* may be synonymous

with either *Yumenornis* or *Jiuquanornis*. Although we recognize these limitations and acknowledge that in the future some names proposed herein may be reduced to junior synonyms, we choose to erect names for specimens that are distinct from other currently available materials.

Among the six new skull-bearing specimens, three different dentary dentitions are present, strongly suggesting that at least three distinct taxa are present in the assemblage. At least one specimen (IVPP V26196) can be differentiated from *G. yumenensis* based on the morphology and proportions of its cervical vertebrae. However, the rostrum is not preserved except as an impression in that specimen, preventing comparison with the three skulls that preserve different dentitions. Limitations relating to differences in the preserved materials and exposed views further complicate attempts to compare the six new specimens. Here, we describe all six specimens, compare the cranial morphologies of these specimens to those of the purported close relatives of *G. yumenensis* – *Iteravis* and *G. zheni*, and explore the phylogenetic position of these specimens through cladistic analysis.

Institutional abbreviations: AGB, Anhui Geological Museum, Hefei, Anhui Province, China; BMNH-Ph, Beijing Museum of Natural History, Beijing, China; CAGS, Chinese Academy of Geological Sciences, Beijing, China; and IVPP,

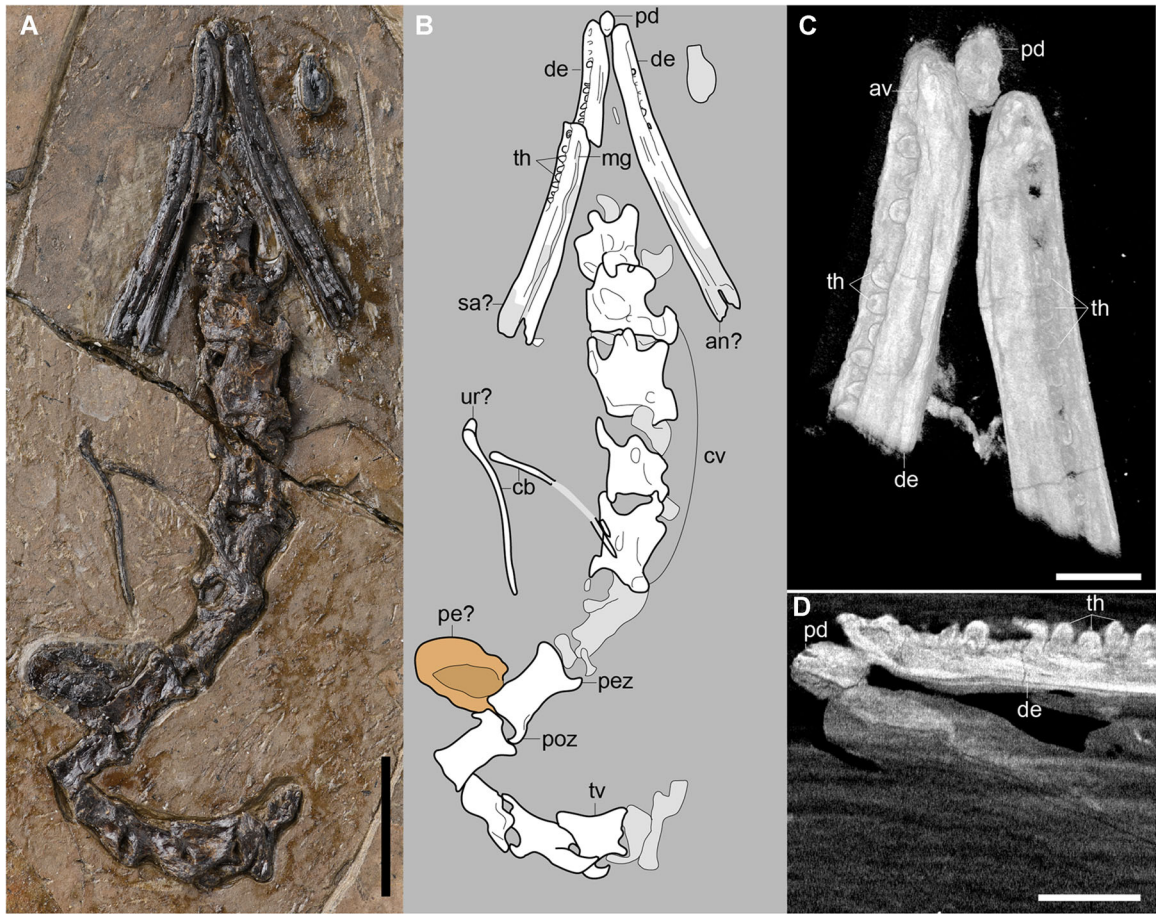


Fig. 4. Holotype of *Brevidentavis zhangi* gen. et sp. nov. (IVPP V26197). **A**, Photograph. **B**, Interpretive drawing primarily in dorsal view. Scale bar equals 10 mm. **C**, Computed tomographic images of dentaries in dorsomedial view. **D**, Computed tomographic images of dentaries in left ventrolateral views showing absence of interdental bone. Scale bars in equal 2 mm.

Institute of Vertebrate Paleontology and Paleoanthropology, Chinese Academy of Sciences, Beijing, China.

Anatomical abbreviations (figure key): am, ampullae; an, angular; ar, articular; as, anterior semicircular canal; at, atlas; av, alveolus; ax, axis; cb, ceratobranchial; bo, basioccipital; bs, basisphenoid; cd, carotid process; cf, carotid foramen; cv, cervical vertebrae; db, depressions on basisphenoid; de, dentary; eb, ethmoid bone; eo, exoccipital; fm, foramen magnum; fr, frontal; ft, feathers; hp, hypapophysis; hy, hyoid element; is, interorbital septum; jg, jugal; mc, mandibular cotyla; me, mesethmoid; mg, Meckel's groove; mm, medial mandibular process; mx, maxilla; na, nasal; nf, nerve foramina; ns, neural spine; pa, parietal; nvf, neurovascular foramen; oc, occipital condyle; od, odontoid process; pb, postorbital process; pd, predentary; pe, pellet; pez, prezygapophysis; pl, palatine; pm, premaxilla; poz, postzygapophysis; pp, paroccipital process; pr, parasphenoid rostrum; ps, posterior semicircular canal; pt, pterygoid; qd, quadrate; ra, retroarticular process; ri, rib; rl, rostralateral foramina; sa, surangular; sg?, possible salt gland; so, supraoccipital; sr, scleral ring; tf, tympanic fenestra; th, teeth; tn, transverse foramen; tv, thoracic vertebrae; ur, urohyal; vf, vein foramen; vm, possible vomer; and?, denotes uncertainty in the identification.

2 Material and Methods

All six specimens (IVPP V26194, V26195, V26196, V26197, V26198, and V26199) are reposit at the IVPP. IVPP V26199 and V26198 were scanned using an industrial computed tomography (CT) scanner Phoenix v/tome/x at the IVPP with a voxel size of 18.86 and 17.61 μm , respectively. IVPP V26197 was scanned using 225 kv micro-CT (developed by the Institute of High Energy Physics, Chinese Academy of Sciences) at IVPP at a voxel size of 7.84 μm . Scans were processed using the software Avizo (v9). Anatomical nomenclature primarily follows Baumel & Witmer (1993), using the English equivalents of the Latin terminologies.

3 Results

3.1 Systematic paleontology

AVES Linnaeus 1758, ORNITHUROMORPHA Chiappe 1999 [sensu O'Connor et al., 2016]

3.1.1 *Meemannavis ductrix* gen. et sp. nov.

Holotype specimen IVPP V26198, poorly preserved partial premaxillae and a possible maxilla and quadrate, a few possible palatal elements, complete orbital region and

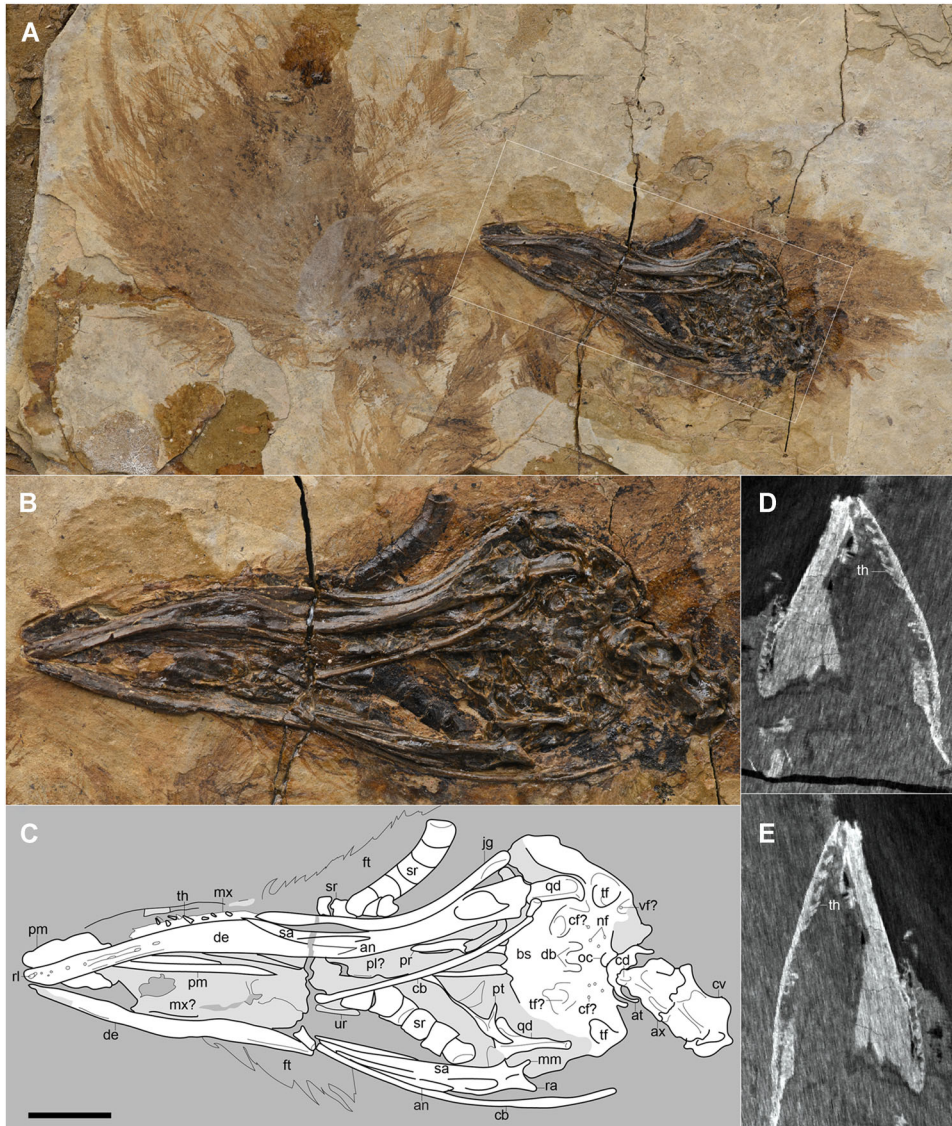


Fig. 5. Referred specimen cf. *Gansus yumenensis* (IVPP V26199). **A**, Photograph of entire specimen, showing extensive feather preservation. **B**, Photograph of skull and cranial cervical vertebrae, primarily in ventral view. **C**, Interpretive drawing of **B**. Scale bar equals 10 mm. **D**, and **E**, Computed tomographic slices revealing the presence of teeth in the dentaries.

braincase prepared free from the sediment, nearly complete and articulated mandible, and partially articulated cervical and thoracic vertebrae preserved together with many small, unidentifiable, disarticulated fragments; bones are in various views and observations are obscured by a thick layer of applied consolidant (Fig. 3).

Locality and horizon Changma township, Yumen City, Jiuquan area, northwestern Gansu Province, China; Lower Cretaceous Xiagou Formation (lower Aptian).

Etymology The generic name is in honor of the paleontologist Chang Meemann (张弥曼; also transliterated as Zhang Miman), -avis, Latin for bird; the epithet “ductrix,” Latin meaning female leader, is in honor of her role as the first woman to serve as director of the IVPP (1984–1990), as a leader in her field in the study of fossil fish, and her role as

mentor, role model, and inspiration to female scientists worldwide.

Diagnosis Medium-sized ornithuromorph bird with the unique combination of the following features: premaxilla corpora fully fused; edentulous dentary that is dorsoventrally shallow, gently curved, and that gradually tapers rostrally; quadrate cotyles of the mandible rostrocaudally narrow. Can be differentiated from other Early Cretaceous ornithuromorphs with edentulous dentaries through the following morphologies: lacks the rostroventral expansion of the dentary seen in *Archaeorhynchus* and overall the dentary is more elongate in *Meemannavis*; mandibular symphysis that is present in *Eogranivora* is absent; dorsal surface of the dentary is gently concave (ventral surface gently convex), whereas it is straight in *Xinghaiornis*.

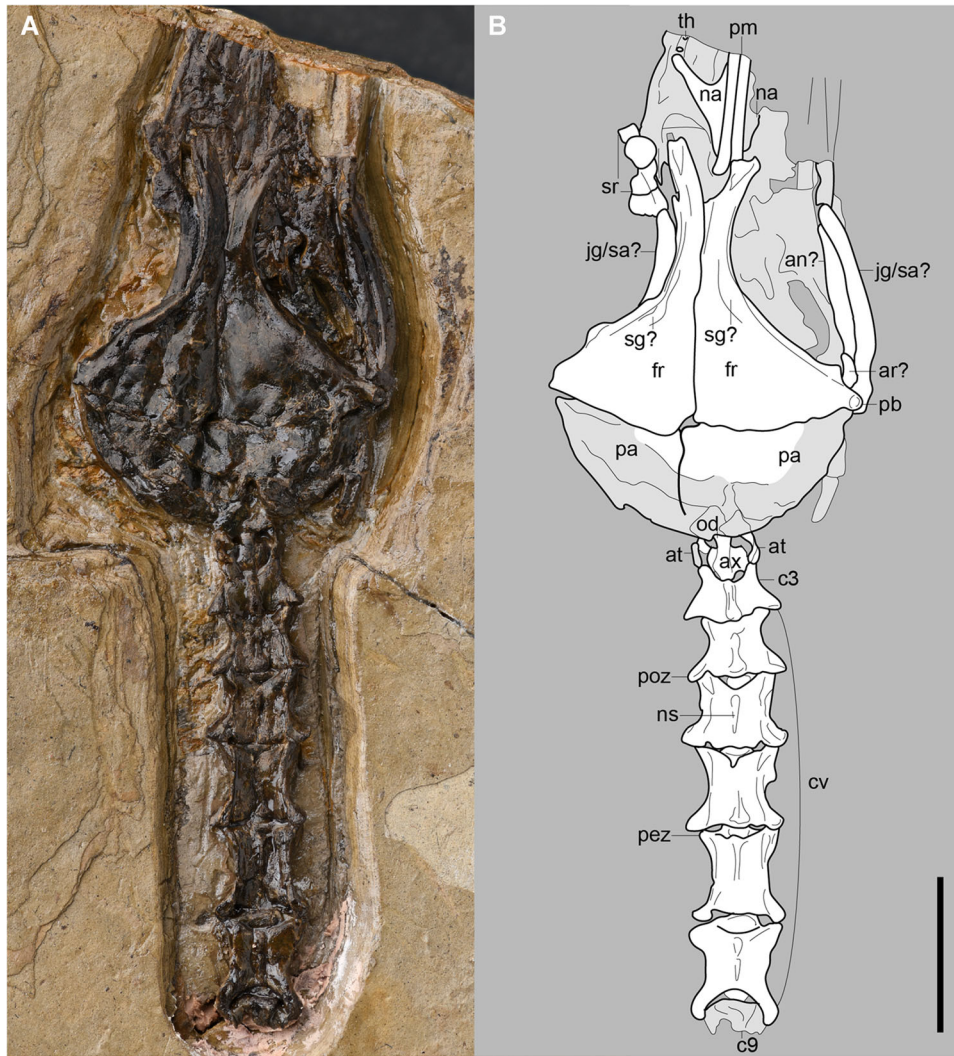


Fig. 6. Specimen referred to *Ornithuromorpha* indet. A (IVPP V26194). **A**, Photograph. **B**, Interpretive drawing in dorsal view. Scale bar equals 10 mm.

Description

Cranium. The premaxillae are flattened into two dimensions and exposed in dorsal view, missing their most rostral tip and the right maxillary process (Fig. 3). The premaxillary bodies are fully fused and edentulous. Only the bases of the frontal processes are preserved with the premaxillary bodies; the main portions of these processes are broken off and displaced to the right. The right and left frontal processes are tightly articulated, but can be distinguished from each other, indicating they are unfused. They taper to blunt ends caudally, and their length suggests that they would have contacted the frontals. As preserved, the left maxillary process comprises half the preserved length of the premaxillary body. In dorsal view, the lateral margins of the premaxillary bodies converge rostrally, demarcating an angle of approximately 26°.

Preserved to the left of the fused premaxillary bodies is what appears to be a long, flat, triradiate element, which may in fact represent two overlapping elements. We suggest this may represent the left maxilla in palatal view, or

alternatively the vomer, or partial maxilla overlapping the vomer. The bluntly tapered (probably rostral) end of this element is just overlapped by the premaxillae. The opposite, wider (probably caudal) end consists of two elongate processes; one slightly longer than the other, separated by a deep, V-shaped notch. If identification as the maxilla is correct, these two elongate processes represent the articulations for the jugal and palatine. Alternatively, the longer process is identified as a palatine underlying a partial maxilla. Along the margin of the side bearing the shorter process, several circular openings are visible; these may be alveoli, which indicate that the tomial margin of the maxilla is exposed. The openings seem proportionately large for alveoli considering the size of the maxillary teeth of IVPP V26199 (see below), but they may be exaggerated by crushing. Similar, proportionately large maxillary alveoli are present in *G. zheni* BMNH-Ph1342.

Two elongate elements are preserved in contact with each other ventral to the postdentary bones. These are connected by an intervening fragment that may be a broken piece of

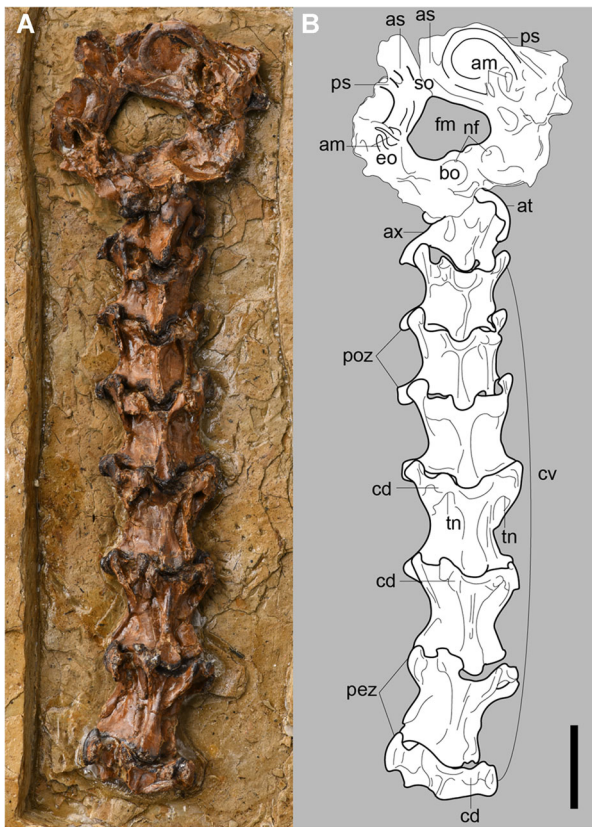


Fig. 7. Specimen referred to *Ornithuromorpha* indet. B (IVPP V26195). **A**, Photograph. **B**, Interpretive drawing primarily in ventral view. Scale bar equals 5 mm.

the more rostral element or a quadrate. The longer element, which parallels the postdentary bones, is tentatively identified as the left pterygoid in dorsal view. The lateral margin is broadly concave; the medial margin is convex overall, formed by two weakly concave sections that meet at the mediolaterally expanded midpoint of the element. The bluntly tapered rostral half of the bone is narrower than the caudal half. The end that articulates with the intervening fragment is expanded, but the precise morphology of this contact is obscured by an overlying bone fragment.

This intervening bone is shaped like an inverted L, with the shorter process in line with the bone tentatively identified as the pterygoid and the longer process oriented at a 90° angle laterally. The fragment could be either the quadrate wing of the pterygoid or the quadrate itself. In the former interpretation, the laterally oriented portion represents the quadrate wing, giving the pterygoid a morphology somewhat similar to that of *Archaeopteryx* (Elzanowski & Wellnhofer, 1996). If correct, the quadrate wing is much more laterally oriented in IVPP V26198 compared to the caudolateral orientation in *Archaeopteryx*. Alternatively, if this bone is the quadrate, the elongate ramus would be its shaft exposed in rostral view but broken such that the orbital process is not preserved.

The second elongate element is preserved parallel to and in contact with the longer process of the possible quadrate. The entire margin of this second element that faces the

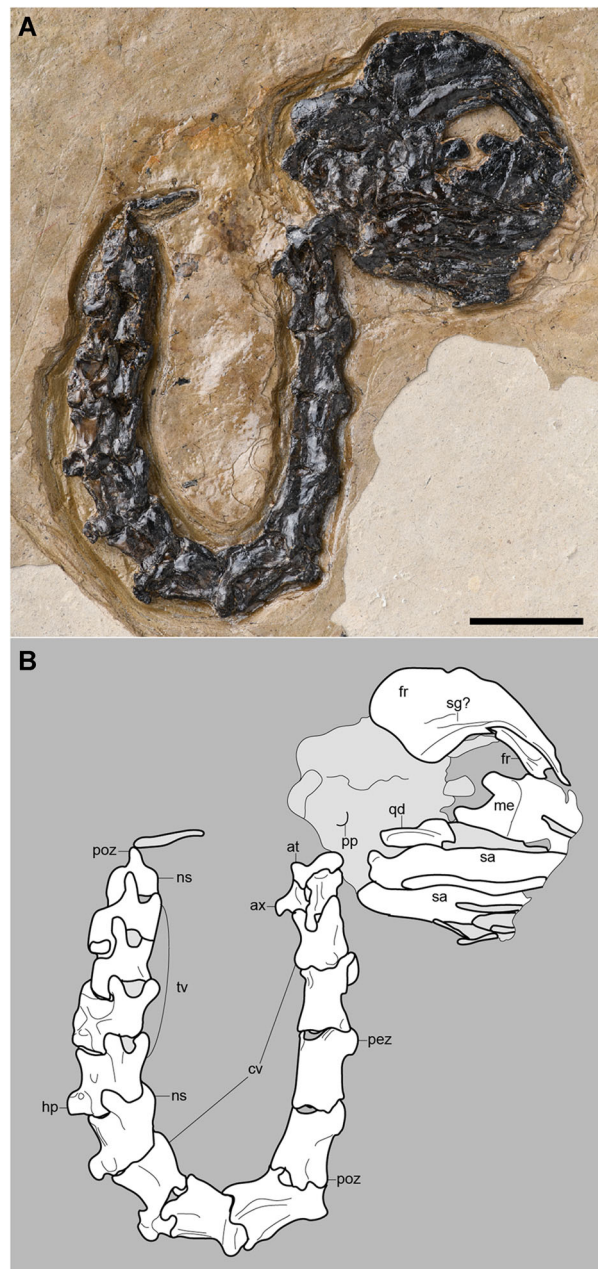


Fig. 8. Specimen referred to *Ornithuromorpha* indet. C (IVPP V26196). **A**, Photograph. **B**, Interpretive drawing in right lateral view. Scale bar equals 10 mm.

possible quadrate is broadly convex. The opposite margin is concave along the narrow portion that makes up the two-thirds of its length oriented toward the possible quadrate and convex along the remaining one-third, which expands gradually into a fan-like structure away from the tentatively identified quadrate. The broadly convex margin forms a low, blunt ridge along the expanded portion of this bone. This element may be a displaced, partial palatine. A similar ridge is present on the dorsomedial margin of the palatine of *Hesperornis* (Elzanowski, 1991).

A long (20.6 mm) and narrow (2.2 mm), isolated element is preserved caudal to the mandible and dorsal to the cervical

vertebrae. This may be either a palatine (based on gross morphological similarity to the palatine of *Hesperornis*) (Elzanowski, 1991) or a prearticular (based on gross morphological similarity to the prearticular of *Archaeopteryx*) (Elzanowski & Wellnhofer, 1996). The half of the bone oriented toward the rest of the cranial elements is waisted so that both sides are concave before expanding briefly and then terminating in a short taper. This half of the bone is poorly preserved and its margins are visibly abraded, such that its true morphology is unclear. The opposite half of the element, oriented away from the cervicals, is widest at its midpoint but curves and gently tapers. This half of the element is thickened, forming a low ridge, as observed in the other putative palatine.

Although prepared free of sediment such that the left and right sides can both be observed, the braincase is transversely crushed almost completely flat – only thicker, more robust elements and portions of elements, such as the occipital condyle, retain significant three-dimensionality. As a result, individual bones and most sutures between them are difficult to unambiguously discern, if indeed these bones were not fully ankylosed. As in other ornithuromorphs, the frontals are elongate and petal-shaped, with mediolaterally narrow rostral portions that expand caudally to their maximum widths caudal to the orbit. A concave, somewhat linear, and mediolaterally oriented (though dorsoventrally oriented in this flattened specimen) groove visible on both sides may be the frontoparietal suture or contact. A distinct postorbital process, like that observed in IVPP V26194 (see below), does not appear to be present.

The left side of the fragment, on which the consolidant was applied, offers little discernible morphological detail, but it bears a neurovascular foramen positioned slightly rostradorsal to the occipital condyle. A dorsoventrally oriented, elongate element appressed to this side may derive from the hyoid apparatus. At least a partial interorbital septum, represented by some fragments in that area, appears to have been present. The gaps in bone coverage at the caudal end of the orbit may be remnants of the optic and other cranial nerve foramina.

The reniform to somewhat crescentic occipital condyle is exposed on the right and caudal surfaces of the specimen. Just rostradorsal to the occipital condyle on the right side is a neurovascular foramen that likely corresponds to that visible on the left side. Rostral to that foramen are two additional foramina aligned dorsoventrally (on this flattened specimen; they likely originally faced ventrally). The more dorsal of the two foramina (possibly for the internal carotid artery) is larger than the more ventral foramen. These foramina and their positional relationships appear similar to the arrangement observed in the undistorted surface of the basicranium exposed in IVPP V26199. Dorsal to that larger foramen is a lateral protrusion of bone that is connected to a raised rim that circumscribes a deep, subcircular, and (currently) laterally directed fossa. That fossa may have been part of the caudal tympanic recess, tympanic cavity, or possibly even the otic cotyle for the quadrate (and dorsal tympanic recess). It also may correspond to the subcircular fossa on the ventral surface of the cranium present in IVPP V26199. This fossa lies near the rostroventral “bottom” of an arc of what is likely the posterior (caudal) semicircular canal

impression (because it is on the caudal surface and extends around the region of the foramen magnum) visible on the dorsolateral aspect of the skull. If correctly identified, this fossa is positioned where the inner ear should be. Near the dorsal apex of the posterior semicircular canal arc is a small, dorsally extending convexity that could be the branching connection of the anterior (rostral) semicircular canal, but this identification is equivocal. The rostral edge of the laterally directed process and rim of the fossa form a rostrally concave margin. That margin overhangs the adjacent bone and may be either the otic cotyle for the quadrate, or possibly, the rostral tympanic recess (with its eustachian tubes).

Mandible. All, or nearly all, mandibular bones are preserved. The right half of the mandible is preserved in articulation, but the postdentary bones appear fragmented and are difficult to interpret. No prementary is preserved. This absence may be real because a prementary has never been documented in an edentulous ornithuromorph, and therefore it may be lost at some point in the evolution of an edentulous rostrum (whether *Meemannavis* had maxillary teeth or was completely edentulous is unclear).

The left dentary is exposed laterally and the right dentary medially or dorsomedially. The rostral ends of the dentaries are unfused. In profile, each dentary is slender and has gently concave dorsal and convex ventral margins that taper rostrally. The ventral margin becomes slightly concave caudally. The lateral surface of the rostral end of the left dentary preserves a small concavity that we identify as the rostralateral foramen, as also observed in IVPP V26199 (see below) and *Yanornis* (Bailleul et al., 2019a). Caudal to this foramen, the lateral margin is grooved for more than two-thirds of its length, but this groove is exaggerated by crushing. The dorsal margin of the dentary above the groove undulates weakly. Caudal to the groove, the dentary increases in dorsoventral height until it reaches the rostradorsal end of the articular surface for the postdentary bones, at which point the dorsal margin slopes ventrally, forming an articulation with the dorsally overlapping surangular. The caudal end appears unforked, but it is possible that a small dorsal process may have been broken away. The medial surface of the dentary, exposed on the right side, is less clear, but it also appears to be grooved. The surface may be obscured by an overlapping splenial, but this is unclear.

The dentaries appear to be edentulous, a condition confirmed by CT scans, which reveal the absence of both teeth and alveoli (Fig. 3). However, in the central region of the left dentary and the caudal region of the right dentary are several evenly spaced, tooth-like objects that have extremely high densities, appearing bright white in the scans. The high-density objects are proportionately very small and located too far caudally in the mandible to be teeth. Their unusually high density relative to the rest of the bone and the absence of clear alveoli and root structures are also not consistent with identification of these structures as teeth. Several other high-density regions extend longitudinally along the ventral margin of the left dentary, the dorsal and ventral margins of the caudal portion of the right dentary, and along the margin of the right premaxillary corpus (Fig. 3).

The dentary is longer than the postdentary bones. A fragment identified as the articular preserves a narrow mandibular cotyle for which the articular surface appears to be mediolaterally wide and rostrocaudally narrow; the ventromedial margin of the cotylar labrum expands medially. The rostral margin of the mandibular cotyles appears to slant caudodorsally so that the rostral margin overhangs the cotyles. The preserved morphology suggests that the mandibular cotyles were not divided into distinct medial and lateral facets, similar to the condition in enantiornithines, but unlike the clear division in neornithines (crown birds). No retroarticular process is observed, but is it unclear whether it is truly absent or if this process is broken or otherwise obscured.

Vertebrae. The remains of at least 12 vertebrae are preserved. A single, isolated thoracic vertebra is preserved a short distance adjacent to the most cranial articulated series of five cervical vertebrae. Caudal to the articulated series are another three articulated cervical vertebrae. Subsequent vertebrae are disarticulated and fragmented. A few fragments interpreted as pertaining to thoracic ribs are also preserved with these caudally located vertebral fragments.

The most cranial five articulated cervical vertebrae are exposed in ventrolateral view. Both carotid and costal processes are visible. The ventral surfaces of these vertebrae appear weakly keeled. The third and fourth vertebrae are longer than the first and second. The more caudal three articulated cervical vertebrae appear to be exposed in ventral view and have short, fused costal processes. The most caudal complete vertebra is identified as a thoracic in ventral view. Its transverse processes are approximately two-thirds the width of the centrum, and the postzygapophyses are large and caudolaterally oriented.

3.1.2 *Brevidentavis zhangi* gen. et sp. nov

Holotype specimen IVPP V26197, both dentaries in dorsomedial view in articulation with the prementary, a pair of hyoid bones disarticulated away from their *in vivo* position, and approximately 12 articulated vertebrae exposed primarily in lateral view. A possible alimentary pellet is preserved partially overlain by the seventh preserved vertebra (Fig. 4). Note that prior to this current in-depth study, this specimen was attributed to *Gansus yumenensis* in a paper that focused on the avian prementary (Bailleul et al., 2019a).

Locality and horizon Changma township, Yumen City, Jiuquan area, northwestern Gansu Province, China; Lower Cretaceous Xiagou Formation (lower Aptian).

Etymology The generic name in Latin meaning short (brevis) tooth (dens) bird (avis) refers to the morphology of the dentary teeth; the specific epithet is in honor of Professor Zhang Xing (张行, formerly of the Gansu Provincial Museum), co-leader of the 2002 expedition that rediscovered the Changma locality.

Diagnosis Small-sized ornithuromorph bird with the unique combination of the following features: prementary present; dentary teeth located in a communal groove with interdental plates absent; teeth brachydont, approximately equal in crown height and mesiodistal length; and dentary teeth

closely spaced, separated by a distance less than half their mesiodistal diameter. Can be differentiated from other ornithuromorphs in which the dentary teeth occur in a communal groove (hesperornithiforms) based on size (*Brevidentavis* much smaller), the morphology of the dentary teeth (crown morphology proportionately taller, recurved, and sharply tapered in hesperornithiforms), and the length of the tooth row (proportionately shorter and with fewer teeth in *Brevidentavis*).

Description

Mandible. The prementary is a small, dorsally exposed, ovoid element preserved in contact with the rostromedial margins of the dentaries. Both dentaries are dorsomedially exposed. Their caudal margins are truncated at approximately the same position. The preserved caudal margin on both sides bears a short incision that divides the caudal portion of the dentary into two short, subequal processes, the more dorsal of which is the more robust. The rostral portions of the postdentary bones also are probably preserved at least partially fused to the dentary, but their contacts are obscured by consolidant applied to the fossil. The medial surface of the caudal two-thirds of each preserved mandible bears a deep, longitudinal groove that we interpret as Meckel's groove. As in neornithines, this groove is well caudal to the rostral tips of the dentaries.

The dentigerous margins of the dentaries are exposed, revealing numerous teeth located in a groove, similar to the condition in Hesperornithiformes. Interdental plates consequently appear to be absent. As in *Hesperornis*, a single alveolus appears to be located rostral to the groove (Dumont et al., 2016). As in *G. zheni* (Liu et al., 2014), the rostral tips of the dentaries are edentulous, marked by a shallow depression (Fig. 4C). Fifteen teeth are preserved on the left side, but more were present, evident from the empty positions within the tooth-bearing groove. We estimate 20–21 teeth were originally present on each side. The teeth are closely spaced: the distances between them are between one-fifth and one-half the mesiodistal diameters of the teeth. Although obscured by the dorsomedial exposure of the dentary, tooth crown height appears to be one-third the height of the dentary. Most of the teeth are broken at the root in the right dentary, suggesting that the teeth were delicate. The few complete teeth are low crowned, blunt, and rounded (dome-shaped): the crowns are roughly equal in apicobasal height and mesiodistal length. Thus, they are distinct from the sharp, slender morphology of the preserved maxillary teeth of IVPP V26199 (see below) and the maxillary and dentary teeth in *Iteravis* and *G. zheni* (Liu et al., 2014; Wang et al., 2018b). The cross-sections of the teeth are circular, as confirmed in CT scans (Fig. 4C).

Two hyoid bones – identified as the ceratobranchials – are clearly preserved in IVPP V26197. They are bowed, similar to those of IVPP V26199. This curvature is more distinct in the rostral halves of each element. The rostral ends are preserved close together; their caudal ends diverge. The blunt rostral ends expand, suggesting the presence of a urohyal. The caudal ends are tapered. A small, suboval piece of bone is preserved near the rostral end of one of the ceratobranchials that may be either the basihyal or the urohyal.

Vertebrae. The remains of approximately 12 vertebrae are preserved (Figs. 4A, 4B). It is unclear if the first preserved vertebra is the axis. The most cranial three vertebrae are poorly preserved. The fourth and fifth are exposed in dorsal view. These preserve elongate, dorsally flexed prezygapophyses that are cranially oriented and only slightly laterally splayed. In contrast, the postzygapophyses are strongly caudolaterally oriented. A delicate and low neural spine is visible on the fifth preserved vertebra. The seventh preserved vertebra is the most elongated.

Additional remains. A small (8.3 mm × 6.3 mm; true dimensions are obscured by an overlapping cervical vertebra), flat, oval mass of dark, carbonized matter is preserved adjacent to, and partially overlapped by, the seventh preserved vertebra (Figs. 4A, 4B). Within this thin mass is a smaller (4.5 mm × 2.3 mm) mass that projects from the slab. Both masses are asymmetrical, with their wider ends underlying the vertebra. Potentially this object may be the remains of an alimentary pellet in the esophagus. However, pellets typically consist of hard-to-digest material, such as bones, hair, and feathers, and such traces are not clearly present in this small, dark mass. It is possible that the pellet consists of feathers; grebes intentionally ingest feathers to improve digestive efficiency, later egesting these feathers as part of a bolus also containing undigestible remains (Jehl, 2017). Given what remains of fossil feathers is typically only the preserved melanosomes, preservation of feathers compacted into a pellet may appear as only a dark residue of fossilized melanosomes. Unfortunately, because this specimen has been designated as a holotype, destructive sampling to confirm the preservation of melanosomes is not possible.

3.1.3 cf. *Gansus yumenensis*

Specimen IVPP V26199, a nearly complete skull, ventrally exposed, in articulation with the most cranial three cervical vertebrae. Numerous associated feathers are preserved both around the skull and in large patches nearby (Fig. 5).

Notes We tentatively refer this specimen to *G. yumenensis* based on similarities with *Iteravis* and *G. zheni* (see Discussion).

Description

Cranium. The premaxillae are exposed in ventral view (Fig. 5). The bodies of the premaxillae are completely fused medially and edentulous. The lateral margins of the short premaxillary body are uneven, suggesting some breakage. The maxillary processes are missing. The premaxillary contribution to the facial margin rostrally comprises 25% or less. Exposed just medial to the left dentary and lying approximately along the skull midline are a pair of flat, elongate bones that tightly articulate medially. The area between these bones and the premaxillary body is covered by the left dentary. However, CT data reveal that these are the unfused frontal processes of the premaxillae. The caudal margins of these bones are broken, but they appear to extend caudally at least beyond the level of the rostral margin of the jugal. Palatal processes of the premaxillae are absent as in *Iteravis*, *Ichthyornis dispar*, and *Gobipteryx minuta* (Chiappe et al., 1999; Liu et al., 2014; Field et al., 2018). The median ridge that is inferred to have supported the

unmineralized internarial septum in *Ichthyornis* (Field et al., 2018) is also absent (Fig. 5).

On the left side, lateral to the dentary and rostral to the jugal, the tomial margin of the left maxilla is faintly visible, exposing alveoli and fragments of small, sharply pointed, conical teeth that together indicate the presence of 10–11 maxillary teeth. Eleven alveoli are also visible in the maxilla of *G. zheni* BMNHC-Ph1342. In IVPP V26199, each tooth appears to be roughly three times taller than its maximum diameter. An extensive, thin sheet of bone medial to the right dentary is interpreted as the poorly preserved palatal process of the right maxilla. This sheet of bone is relatively flat, and its caudal end lies at nearly the same level as the most distal maxillary tooth.

The ventrolaterally exposed left jugal is preserved in articulation with the maxilla and appressed to the lateral surface of the postdentary bones. The rostral 40% of its length has a ventral facet that suggests a long, overlapping articulation with the maxilla. The jugal is bowed, rendering its dorsal margin weakly concave. The blunt caudal margin appears to lack a dorsal postorbital process. The quadratojugal is not visible as a distinct, separate bone and may be fused to the jugal.

Both the left and right quadrates are preserved, exposed in caudal and caudolateral view, respectively (Figs. 5A–5C). The caudal margin of the quadrate forms a relatively mediolaterally thin, dorsoventrally straight column. The rounded, bulbous, and undivided otic head is enlarged relative to the narrow caudal margin, and is expanded medially, overhanging the otic process. The orbital process appears to extend ventrally from the otic head (visible on the left side). The ventral extent is unclear, but it appears to have at least approached the mandibular condyles of the quadrate. Dorsally, the articular surface of the otic head extends rostrally as a mediolaterally expanded dorsal edge of the orbital process. Most of the lateral surface of the orbital process appears to be nearly flat except for its dorsal end where it is increasingly concave adjacent to the otic head. The dorsal part of the rostral edge of the orbital process might have been somewhat thickened relative to its more ventral edge. The mandibular region of the quadrate is not exposed on the left side (covered by the lower jaw) and this region is broken and partially covered on the right quadrate. However, the mandibular region is clearly mediolaterally expanded. Its preserved morphology suggests that the lateral condyle was wider than the medial condyle, but the extent of the latter is not clear. A fragment of bone located between the base of the medial mandibular process of the right quadrate and the right mandible may belong to the lateral mandibular condyle. A thin, flattened piece of bone that likely is part of the pterygoid overlaps much of the medial surface of the ventral part of the right quadrate, suggesting an expanded contact between the pterygoid and quadrate.

The braincase is exposed ventrally and crushed flat, making interpreting the exact relationships among the preserved elements difficult. The ventral portion of the occipital condyle is exposed, preserved in articulation with the atlas. This orientation strongly suggests the foramen magnum was caudally oriented as in other Cretaceous non-ornithine birds. Lateral to the occipital condyle on both

sides, exit foramina likely for three cranial nerves (X–XII) are clearly visible. The caudal two foramina, likely those for cranial nerves XI and XII, are positioned roughly mediolateral to one another near the caudal edge of the skull. A fourth foramen on the left side that lies rostralateral to the other three foramina may be for entry of the internal carotid artery. Lateral to these foramina on each side is a large fossa with a rounded, subtriangular margin (with a caudally directed apex and a more rounded rostral margin). Given their positions caudal to the otic articulation of the quadrate, these depressions may be the caudal tympanic recesses. Each fossa is deepest caudally, shallowing rostralaterally. The caudal apex of each lateral fossa is caudal to the occipital condyle, suggesting that the caudal margin of the skull (in dorsal or ventral view) may have been concave caudally, as in some extant birds (e.g., pelicans). A shallowly concave area caudomedial to the presumed left caudal tympanic recess may represent the exit of a vein (Fig. 5).

Rostromedial to these recesses on the basisphenoid plate are two similar but smaller and shallower depressions that may be either openings of the rostral tympanic recesses or the openings of the auditive (eustachian) tubes. These recesses are rostral to the groups of nerve foramina described above, lying near the rostral edge of the basisphenoid plate. The subcircular margins of the recesses have distinct, thin, raised rims (Fig. 5).

The rostral edge of the basisphenoid plate is not clearly preserved, but the midline region of the basisphenoid is broadly concave (rostral to the nerve foramina and overlapping with the possible rostral tympanic recesses), but with what appears to be a low, rostrocaudally oriented division of the concavity that separates it into left and right sides. The subcondylar fossa is small and shallow.

Parts of the palate are exposed. The elongate parasphenoid rostrum is visible extending rostrally, but it is overlain by the left post-dentary bones and ceratobranchial, obscuring the most rostral portion. A thin bone interpreted as the right pterygoid is preserved overlapping the mandibular region of the right quadrate. It is angled ventromedially–dorsolaterally. Its caudal end, in contact with the quadrate, is ventrally expanded where it overlaps the medial part of the latter bone. An additional process of the pterygoid extends medially from this junction. Its articulation with the parasphenoid rostrum through basiptyergoid processes or facets is unknown.

A poorly preserved element, to the right of the parasphenoid rostrum and overlapped by the left ceratobranchial, may be the right palatine. The rostral end of this element approaches the caudal portions of the frontal processes of the premaxillae. The rostral half of this element appears to be a compressed sheet of bone that presumably has been disarticulated so that, as preserved, it is angled ventrolaterally–dorsomedially. The caudal half of this element appears to be forked, with the medial process contacting the parasphenoid rostrum just rostral to its midpoint, and the longer lateral process contacting the parasphenoid rostrum at its base. Near its midpoint, the element contacts the pterygoid. None of these contacts is interpreted as indicative of the *in vivo* condition.

The ventral one-third of the scleral ring is preserved on both sides, each preserving six ossicles in articulation,

including one underplate. Several other broken and disarticulated ossicles also are preserved on the left side. The lateral surfaces of the ossicles are convex. The outline of each individual ossicle is nearly square, and the margin overlapping the adjacent ossicle is broadly convex. When in articulation, the internal margins that enclosed the pupil are shorter than the external margins. The margin typically overlapped by the adjacent ossicle, exposed in the last ossicle in the articulated series on each side, bears an articular facet that is wider toward the interior and tapering at the exterior margin.

Mandible. The left dentary is ventrolaterally exposed, and the right dentary is in ventromedial view. The rostral ends of the dentaries are unfused, and thus, a mandibular symphysis is absent. The rostral margin slopes rostrorodorsally–caudoventrally. In profile, the slender, rostrally tapering dentary has a gently concave dorsal margin and more strongly convex ventral margin. In the left dentary, the rostralateral foramen (*sensu* Bailleul et al., 2019a, 2019b) for the mandibular nerve is visible, exiting the dentary at its rostralateral extremity, as in *Yanornis* (Bailleul et al., 2019a) (Fig. 5). Eight nutrient foramina perforate the lateral surface caudal to the rostralateral foramen. The rostral three of these foramina are small and circular, the fourth and fifth are larger but still circular, and the caudal three foramina are rostrocaudally elongate. The caudal four foramina are located in a shallow, rostrocaudally oriented groove. The ventral margin of the rostral one-third of each dentary is sharply keeled. In contrast, the ventral margin farther caudally is mediolaterally wider and rounded. The dorsal margin of the caudal one-third of the dentary slopes ventrally, forming a long, unforked overlapping articulation with the surangular. The splenial is not visible on the right mandible, which is ventromedially exposed, suggesting it may be fused to the dentary.

CT scans reveal numerous dentary teeth similar in morphology to the maxillary teeth that are visibly exposed in this specimen. They are small, slender, sharply tapered, and closely spaced. The low quality of the scan images prevents the unequivocal identification of anatomical details, but in at least some areas, interdental bone appears to be absent (Figs. 5D, 5E).

The surangular is only minimally exposed on the right side, with small portions of the ventromedial and ventrolateral margins visible clasping the angular. The rostrally tapered portion of the left surangular is preserved in articulation with the dentary along its ventral surface. Caudally, the surangular and angular cannot be clearly differentiated, suggesting that these two elements were at least partially fused.

The left angular is ventrally exposed rostrally and ventrolaterally exposed caudally. Its rostral end appears to articulate with the most caudal portion of the dentary. In ventral view, the mediolateral width of the rostral one-third of the angular tapers rostrally. Caudally, the angular expands dorsally. The contact between the angular and articular cannot be identified.

The caudal margin of the articular forks into retroarticular and medial mandibular processes, suggesting the presence of a caudal fossa. This morphology is clearest on the right side. While it also is visible on the left side, the retroarticular

process appears to be broken. In ventral view, the medial mandibular processes are roughly triangular. The retro-articular process is short, with a caudal apex that lies somewhat lateral to the mediolaterally expanded articular surface for the quadrate. Rostral to the base of these two processes, another process extends medially, but its morphology is obscured by overlap of the quadrate. The lateral surfaces of both articulars are excavated by fossae that shallow rostrally, but in each case, the precise morphology is obscured by crushing.

As in most Cretaceous birds, only two hyoid bones, the ceratobranchials, are clearly preserved. The rostral ends are preserved in close proximity, though their bodies diverge caudally. They are long, over half the length of the mandible, and weakly bowed such that the dorsal surfaces are concave. Their rostral extremities have small, bulbous expansions that indicate that they likely articulated with an unpreserved, and probably unossified, epibranchial. The caudal end of the right ceratobranchial is not preserved. In cross section, the ceratobranchials appear to change from a dorsoventrally elongate oval rostrally to a subcircular morphology caudally. A rostrocaudally elongate and mediolaterally narrow fragment of bone that extends caudally from the preserved rostral apex of the left ceratobranchial is consistent in morphology, relative size, and anatomical position with identification as the urohyal.

Cervical vertebrae. The ring-shaped atlas, preserved in articulation with the occipital condyle, is exposed in caudal view (Figs. 5B, 5C). The articular surface for the axis projects from the body of the atlas. The atlantal arches are mediolaterally compressed where they form the lateral margins of the neural canal and become more delicate dorsally. The dorsal margins of the atlantal arches are not exposed.

The axis is ventrolaterally exposed. The articular surface for the atlas has a sagittal, ridge-like ventral projection that is not present in IVPP V26195. The lateral surface of the axis is deeply excavated. The cranial half of the ventral surface of its centrum has a shallow, longitudinal groove, and the caudal half is unclear. The postzygapophyses have craniocaudally elongate articular surfaces that are wider caudally than cranially.

The ventral surface of the first postaxial cervical (C₃) is keeled. The cranial end of the ventral surface, in line with the keel, expands into two small, blunt, tubercle-like cranioventral projections that are tentatively identified as carotid processes. The prezygapophyses are approximately 40% the length of the centrum and expand cranially. The centrum is slightly longer than wide.

Integument. Feathers on the left lateral margin of the skull extend caudally from a point roughly level with the distal margin of the maxillary tooth row (Fig. 5A). These feathers are very short (0.9–2.3 mm), but become progressively more elongate caudally, reaching a maximum preserved length of 20.5 mm along the caudal margin of the skull. The feathers on the right lateral margin of the skull begin 11 mm from the rostral end of the dentary. These measure 4.3–5.6 mm for their entire extent along the right ventrolateral margin.

Adjacent to the rostrum is a large cluster of at least eight long (approximately 40–50 mm) feathers that are connected at their bases, suggesting they may belong to the wing. The basal two-thirds of their lengths are obscured, probably by overlap of a layer of shorter feathers. Additional shorter feathers can be observed extending out to the sides from the base of the cluster. Where not obscured by overlap, the rachises, barbs, and barbules of these feathers are clearly observed. The feathers do not appear to be asymmetrical or to have tightly interlocking barbs in most areas, and thus cannot be primary remiges. Below this large cluster is a smaller clump of feathers, the basal portions of which are cut off by incomplete preservation of the slab (maximum preserved length 26 mm). In some regions, the barbs are clearly preserved interlocking with adjacent barbs.

3.1.4 Ornithuromorpha indet. A

Specimen IVPP V26194, a skull preserving the most caudal portion of the rostrum and the orbital and postorbital regions in articulation with eight complete cervical vertebrae and the cranial portion of another, all elements exposed in dorsal view (Fig. 6).

Description

Cranium. The specimen preserves the caudal portions of the frontal processes of the premaxillae, and these are tightly appressed medially, although unfused, and caudally in contact with the right frontal. On the left side, crushed bone extends from the frontal processes laterally to the level of the preserved scleral ossicles. That crushed bone area likely consists of palatal bones, the left maxilla, and mandibular bones. Overlying these elements is the left nasal. The nasal has three processes: a short and sharply tapered premaxillary process; a long maxillary (descending) process; and the caudally extending nasal corpus, which is sharply tapered. This morphology is similar to those of *Yanornis* (IVPP V13358) and *Hesperornis* (KUVPP 71012). A fragment of the nasal corpus also is preserved on the right. At least one tooth appears present in the most rostral portion of this area of crushed bone. The conical tooth is preserved with its apical tip protruding from the slab, suggesting it is a dentary tooth.

On the right side, an elongate, robust, and weakly laterally bowed element demarcates the ventral limit of the orbit. This bone may be the caudal portion of the right jugal preserved in dorsal view. If correct, the jugal bar is fairly robust, at least relative to the delicate morphology present in *Schizooura* (Zhou et al., 2012). No separate quadratojugal is preserved. Ventromedial to the putative right jugal is a robust, straight bone that likely derives from the mandible. This identification may suggest an alternative interpretation of these two fairly robust elements; namely, that they are the angular and surangular, respectively (in other words, that the potential jugal is actually the surangular). This latter interpretation is supported by the presence of a small bone located at their most caudal exposed portions, which may be the articular. Between these elements and the orbital margin of the right frontal, the orbit is filled with overlapping and fragmented bones of the palate and possibly the lacrimal, mesethmoid, and/or ectethmoid.

The frontals are unfused to each other and to the parietals. They form the dorsal margin of the orbit. The

rostral half of each frontal is mediolaterally narrow; the element expands markedly caudal to the midpoint of the orbit. The rostral margin of each frontal bears a V-shaped, rostrally directed facet that may be for articulation with the nasals, as in *Ichthyornis* (Clarke, 2004). The rostral ends of the frontals bend slightly laterally such that they do not contact each other medially along their most rostral portions, similar to the condition observed in hesperornithiforms (Bell & Chiappe, 2020) and *Ichthyornis* (Clarke, 2004). In *Ichthyornis*, the frontal processes of the premaxilla fit into this space (Clarke, 2004). The articulation of the caudal margin of the frontals with the parietals is oriented transversely, and is slightly convex caudally. The orbital rim of each frontal thickens caudally so that the caudal half forms a distinct, ventromedially oriented margin visible in dorsolateral view. Although equivocal due to preservation, medial to the orbital rim and just caudal to the midpoint, there appears to be a weak excavation that may be the supraorbital salt gland fossa similar to that reported in *Iteravis* AGB5841 (Wang et al., 2018b) and also visible in *G. zheni* BMNH-C-Ph1342. The caudolateral margin of the frontal, visible on the right side, expands into a blunt postorbital process. A free postorbital bone is not visible and one has never been identified in an ornithuromorph.

The parietals are not fused to the frontals, nor to each other. They appear to have quadrangular outlines, mediolaterally wider than dorsoventrally tall, but their morphologies are obscured by their caudodorsal exposure.

The remains of four scleral ossicles are preserved in the rostral region of the left orbit. These are roughly square in outline, similar to those of IVPP V26199. Rostrally overlapped by the scleral ossicles, a curved bone exposed in the orbit lateral to the left frontal and caudally overlapped by this element may be the left jugal. It is similar in morphology to the bone tentatively identified as the right jugal.

Cervical vertebrae. Eight complete cervical vertebrae (C1–C8) and the cranial portion of another (C9) are preserved fully articulated and exposed in dorsal view (Fig. 6). The vertebrae have been flattened, rendering them primarily two-dimensional. The cranial articular surfaces of the centra protrude cranially relative to the neural arches. The caudal articular surfaces of the centra appear to have been craniocaudally level with the caudal margin of the neural arch. The cranial and caudal articular surfaces of the centra are not visible. Although in dorsal view, the articulations between the centra are linear rather than arcuate, which may suggest that the vertebrae are not fully heterocoelous, but amphiplatyan or amphicoelous.

The centrum of the atlas is covered by the skull such that only its neural arch is visible, rotated caudally, and exposed in oblique craniodorsal view. The right arch is well preserved, indicating that a continuous atlantal arch was not present, as in IVPP V26195.

The neural arch of the axis is shorter craniocaudally than those of the remaining preserved cervical vertebrae. A pronounced odontoid process (dens) projects cranially, and its tip is hidden beneath a crushed portion of the braincase. A neural spine is absent.

Cervical vertebrae C3 through C8 are all very similar in appearance, and here are described collectively except

where noted. Like the axis, C3–C6 are transversely wider across the postzygapophyses than any other portion of the bone. C3–C5 are transversely wider than craniocaudally long, and farther caudally, this trend reverses such that C6–C8 are longer than wide. The concave lateral margins of the neural arches are smoothly curved from pre- to postzygapophyses with no transverse processes visible.

The neural spines are narrow, low, and elongate, spanning the entire dorsal surfaces of most of the vertebrae (but see below). Caudal to the neural spine of C4 is a shallow sagittal sulcus that may be a caudal elastic ligament fossa, and caudal to that of C6 is a flat, unadorned surface lacking any indication of a broken spinal base. The preserved caudal margins of the neural spines of C4 and C5 are very thin. If any of the spine is broken in this region, it could not have extended much farther caudally. Therefore, the spines of C4 and C5 appear restricted to the cranial halves of their neural arches. Crushing renders all but a small sagittal ridge ambiguous on C6, and some or all of this ridge may constitute the neural spine. C7 bears a similar but much clearer ridge. Its thin but broken edge indicates that the complete neural spine was lower than those of C3–C5.

The prezygapophyses are primarily cranially oriented and only weakly laterally splayed. They become proportionately shorter, more robust, and more craniolaterally oriented in the caudal region of the cervical series. The postzygapophyses are proportionately longer than the prezygapophyses and are strongly oriented laterally such that the lateral margins of the postaxial cervicals are concave in dorsal view, and the distances between the postzygapophyses are greater than those between the prezygapophyses. The lateral concavity is most pronounced in C4. The postzygapophyses of C7 and C8 are longer and more caudally oriented than those of the more cranial cervicals. The caudodorsal margins of the postzygapophyses of C6 and C7 bear small epipophyses (dorsal tori), but no such structures are visible on any other cervicals. C5 and, to a much lesser extent, C4 bear shallow but abrupt notches where the prezygapophyseal rami merge with the base of the neural spine that suggest elastic ligament fossae, but no such structures are evident on the remaining vertebrae.

3.1.5 Ornithuromorpha indet. B

Specimen IVPP 26195, the caudal portion of a braincase with the interior surface exposed such that the raised surface of the labyrinth is visible; preserved in articulation with eight well preserved, ventrally exposed cervical vertebrae including the atlas and axis, plus the cranial portion of the ninth cervical (Fig. 7).

Description

Cranium. IVPP V26195 preserves the bones defining the foramen magnum in rostral (internal) view. The foramen magnum as preserved is shaped like a spade or inverted heart with the apex of the pointed dorsal margin leading to a crack that traverses the midline of the supraoccipital. The dorsomedial margins of the foramen magnum are straight and the ventrolateral margins are strongly concave (internally). The ventral margin of the foramen magnum laterally bears two small, dorsally directed convexities that are separated by a shallow concavity located on the midline. On both sides, rostral and slightly lateral to each of these

convexities, are small fossae with probable foramina in their caudolateral margins, likely for the exit of cranial nerves. These openings most likely correspond to the most caudal, ventral foramina observed in IVPP V26199. A gentle ridge extends along the midline of the basioccipital. The dorsal surface of the basioccipital is concave.

The exoccipitals contain the large posterior (caudal) semicircular canals, which are clearly visible as raised surfaces. The left posterior semicircular canal is nearly complete. Short segments of what appears to be another semicircular canal on each side extend dorsal to the medial edges of the more complete canals. These more dorsally extending canals lie medial to the posterior canals for the parts of their length that lie adjacent to the dorsolateral sides of the foramen magnum, and they separate above the dorsal edge of the foramen magnum. These may be portions of the anterior (rostral) semicircular canals. The broken openings of the posterior canals are clearly visible on the right side in the region interpreted as the exoccipital. Near the ventromedial bases of the preserved semicircular canals are two broken, rostrocaudally elongate openings that may correspond to the ampullae. Lateral to the dorsal edge of the potential ampullae is a deep pit on each side that may relate to the spaces for the lagena, cochlea, or lateral semicircular canal.

Cervical vertebrae. Eight complete, uncrushed cervical vertebrae (C1–C8) are preserved in complete articulation and in ventral view. The cranial end of C9 is also preserved. Only part of the left atlantal arch is visible, mediolaterally compressed at its midpoint. Similar to IVPP V26194, a continuous atlantal arch appears to be absent. The cranial two-fifths of the ventral surface of the axis is rounded, ending in two tubercles, caudal to which the ventral surface is keeled. The caudal half of the ventral keel expands into a tubercle that marks the ventral margin of the caudal articular surface.

The centra appear slightly wider than long in C3–C5, but are longer than wide in C6–C8, similar to the condition in IVPP V26194. The vertebrae are in articulation, so their articular surfaces are mostly obscured. The cranial articular surfaces of C3 and C4 are cranioventrally oriented and mediolaterally wider than dorsoventrally tall. The ventral surfaces of these vertebrae are keeled. The keels become wider, forming distinct ventral surfaces in the following cervicals. These ventral surfaces have slight ridges on the cranial halves in C7–C9. The cranial articular surface becomes more cranially oriented in C4–C9, losing the cranioventral orientation present in more cranial vertebrae. Well-developed carotid processes are present in all postaxial vertebrae on the lateral margins of the cranial articular surfaces. The ventral margins of the caudal articular surfaces all possess caudoventral processes that overlap their respective, succeeding caudal vertebra, suggesting that the cervical vertebrae are heterocoelous.

The prezygapophyses are approximately one-third of the length of the centra in C3 and C4. They are cranioventrally oriented so that the articular surfaces are located lateral to their central bodies and cranial to the cranial articular surfaces of the centra. They become progressively shorter in C5–C9. They have crests (ansae) that extend down their

ventral surfaces connecting to the carotid processes via a bridge of bone that ventrally encloses the transverse foramen. The postzygapophyses are oriented caudolaterally, but are more strongly laterally oriented than the prezygapophyses.

3.1.6 *Ornithuromorpha* indet. C

Specimen IVPP 26196, the orbital and postorbital region of a skull (including caudal portions of the mandible) in articulation with 15 vertebrae exposed largely in right lateral view; a shallow, poorly defined impression of rostral bones (suggesting a long, dorsoventrally narrow rostrum) is visible in the matrix (Fig. 8).

Description

Cranium. The skull bones are crushed flat, and contacts between them are heavily obscured by consolidant. Few anatomical details can be clearly discerned. A sheet of bone visible in the rostral half of the orbit is likely the mesethmoid. The right frontal is in lateral view, and the rostral portion of the left frontal is ventrally exposed in the orbit below the right frontal. The frontals are petal shaped as in other Mesozoic birds, rostrally narrow and caudally expanded. The lateral margins of the narrow, rostral portion of the frontals appear to be ventrolaterally thickened, dorsally enclosing the olfactory tract and bulb. A blunt postorbital process like that of IVPP V26194 appears to be absent. However, similar to IVPP V26194, the caudal half of the orbital rim forms a distinct margin that widens caudally. A groove dorsomedial to the caudal half of the orbital margin may represent a supraorbital salt gland, such as that reported in *Iteravis* AGB5841 (Wang et al., 2018b) and also tentatively identified in IVPP V26194. This margin angles ventromedially from the dorsolateral rim of the orbit. On the caudoventral corner of the skull is what appears to be a rounded paroccipital process of the exoccipital.

The quadrate is disarticulated (dorsoventral axis is now rostrocaudally oriented) and slightly rotated (90° laterally/clockwise along the original dorsoventral axis) so that the orbital process, if not broken, would have been directed out of the slab. The quadrate shaft is mediolaterally wider than the thin shaft exposed in IVPP V26199. The otic head has a relatively flat articular surface and does not appear to be expanded relative to the shaft, but it is mediolaterally broad. A crest, missing some of its extremity, that is likely at least part of the orbital process extends from the otic head ventrally to what appears to be the ventrolateral corner of the bone. The dorsal and ventral areas appear complete with the mid-section broken away (consistent with a dorsoventrally narrowed orbital process). The presumed lateral surface of the crest is deeply concave on its caudal aspect (along the corpus of the quadrate). The crest appears to be rostrocaudally broader in its dorsal portion, and it has a somewhat thickened edge dorsal to its ventral end that appears to mirror the ventral preserved portion. The mandibular region is mediolaterally wider than the dorsal portion, but mandibular condyles are not clearly visible. The otic head is much broader than it is among enantiornithine birds, in which the otic head facet is relatively small and somewhat circular in at least some taxa (e.g., *Rapaxavis*) (O'Connor & Chiappe, 2011). The caudal ends of the

mandibular rami are rounded and appear to lack retro-articular processes.

An impression of the rostrum is preserved suggesting it was narrow and tapered (Fig. S1). Although how the bones of the rostrum were lost is unknown, we suggest one plausible explanation: the bedding of the Xiagou Formation at Changma is largely vertical and slabs regularly become loose and fall to the ground unaided. IVPP V26196 may represent one such slab. The fall presumably caused the bones of the rostrum to break off and, due to their small size, unfortunately they were not recovered with the rest of the specimen.

Vertebrae. Fourteen complete vertebrae, plus the incomplete remains of a 15th vertebra (C15) are preserved in articulation with the skull and each other (Fig. 8). The atlas (C1) and axis (C2) are preserved overlapping and crushed in such a way that anatomical details are unclear. The postaxial vertebrae are preserved in lateral view. C3 is craniocaudally longer than tall. The cervicals elongate caudally through the series, with C5–C7 being the longest. The postzygapophysis of C3 and prezygapophysis of C4 are visible clearly where these two vertebrae articulate. The postzygapophysis is longer than the prezygapophysis, although both extend onto the adjacent vertebrae for approximately one-third the length of the centrum. The articular surface of the prezygapophysis is distinctly angled craniodorsally at an angle of approximately 45°, whereas that of the postzygapophysis appears to be oriented horizontally.

Between C6 and C7, the series twists so that instead of the left lateral surface, the right lateral surface is exposed. The cervicothoracic (CvT) transition is estimated to occur between the ninth (C9) and 11th (T1) vertebrae. No thoracic ribs are preserved, but these three vertebrae have ventral processes (hypapophyses). The 10th (CvT1) has a well-developed neural spine with a deeply concave caudal margin, and this concavity becomes even more pronounced in T1 (11th vertebra in series) and T2. T2 is laterally excavated by a broad fossa that is enclosed cranially by a delicate ridge. T1 bears a similar, but much smaller, fossa.

3.2 Comparisons

Comparisons among the six specimens described here are hindered by differences in preserved elements and their exposed views. For example, IVPP V26194 and V26195 preserve little overlapping cranial material (the caudal portion of the braincase is preserved in both but not exposed in IVPP V26194), but both are associated with well-preserved cervical series. However, in IVPP V26194, the vertebrae are preserved in dorsal view, and in IVPP V26195 they are preserved in ventral view, hindering direct comparison. Premaxillae are partially preserved in IVPP V26194, *Meemannavis* V26198, and V26199, but the premaxillary body is preserved only in *Meemannavis* V26198 and V26199; it is edentulous in both, as in *Iteravis*, *G. zheni*, *Ichthyornis*, and *Hesperornithiformes*. As in *Ichthyornis* and *Hesperornithiformes*, the bodies of the premaxillae are completely fused to one another medially. It is unclear if the premaxillae are fused in *Iteravis* IVPP V18958, but they are unfused in *G. zheni* BMNH-Ph1342. *Gansus zheni* BMNH-Ph1342 was regarded as an adult by the original authors (Liu

et al., 2014) and is the second-largest referred specimen, making it unlikely that the absence of fusion is related to ontogeny. Palatal processes are absent in IVPP V26199, as in *G. zheni* BMNH-Ph1342, *Ichthyornis*, and *Gobipteryx* (Chiappe et al., 1999; Liu et al., 2014; Field et al., 2018), but palatal processes are present in *Hesperornis* (Elzanowski, 1991). The median ridge present in *Ichthyornis* that is inferred to have supported an unmineralized internarial septum (Field et al., 2018) is absent in both *G. zheni* (Liu et al., 2014) and IVPP V26199 (Fig. 5). The frontal processes of the premaxillae are not fused in *Meemannavis* IVPP V26198, V26199, and V26194, as in *Iteravis* IVPP V18958 and *Hesperornis* (Elzanowski, 1991). In the latter taxon, the unfused frontal processes can be traced into the imperforate rostral portion of the premaxilla, suggesting that the expansion of the premaxillary corpus was achieved by ossification of the region between the frontal processes and the maxillary process. These processes are fused only along their rostral halves in *Ichthyornis* (Field et al., 2018), whereas in *Meemannavis* IVPP V26198, V26199, and *Iteravis*, the frontal processes are unfused along their entire post-corporal lengths.

Among the six specimens, the occlusal margin of the dentary is exposed only in *Brevidentavis* IVPP V26197 and *Meemannavis* V26198. In *Meemannavis* IVPP V26198, dentary teeth are absent, as confirmed by CT scans (Fig. 3). Teeth are visible in CT scans of IVPP V26199, revealing their morphology as similar to that of the visible maxillary teeth: small, slender, sharply tapered, and closely spaced (Figs. 5C, 5D). Similar teeth are present in specimens of *Iteravis* (Zhou et al., 2014) (Fig. 2B). A single tooth preserved in IVPP V26194 is tentatively identified as a dentary tooth. To what little extent it can be observed, the tooth is conical and generally similar to those in IVPP V26199. The dentition typically does not vary between the upper and lower jaws in Mesozoic birds, except in *Sapeornis* in which the dentary teeth are vestigial and possibly ontogenetically lost with maturity (Wang et al., 2017a, 2017b). CT scans reveal that the dentigerous margin of the dentary of IVPP V26199 would have occluded with the edentulous premaxilla, as in *G. zheni* (Liu et al., 2014) and the Late Cretaceous ornithurines *Ichthyornis* and *Hesperornis* (Field et al., 2018). In contrast, the teeth of *Brevidentavis* IVPP V26197 are low and blunt, being approximately equal in crown height and mesiodistal diameter (Fig. 4). These teeth are tightly packed and appear to be set in a communal groove and not separated by interdental plates, a condition shared with *Hesperornithiformes* (Dumont et al., 2016). Although less clear due to the absence of CT data, this morphology also superficially appears to be the case for the dentary teeth of *G. zheni* (Liu et al., 2014). However, this observation may simply be the consequence of both poor preservation and the close spacing of the teeth. In the future, this configuration should be confirmed through high-resolution imaging.

The quadrate shaft is wider in IVPP V26196 than IVPP V26199 such that the otic head does not appear expanded relative to the shaft in the former (Figs. 5, 8). A retroarticular process like that present in IVPP V26199 appears absent in IVPP V26196 and *G. zheni* BMNH-Ph1342; the condition in IVPP V26198 is indeterminate.

The hyoid bones of IVPP V26199 are proportionately much longer than those of *Brevidentavis* V26197 (Table 1). Unfortunately, the hyoids of specimens of *Iteravis* and *G. zheni* are not fully exposed, preventing accurate measurements from being collected for comparison. Both IVPP V26199 and *Brevidentavis* V26197 also appear to preserve a urohyal, an element otherwise reported only in *Confuciusornis* and *Hongshanornis* among Mesozoic birds (Zhou & Zhang, 2005; Li et al., 2018). The rostral ends of the ceratobranchials are expanded, suggesting the presence of a basihyal (entoglossal) that was either unossified or not preserved (the basihyal is present in *Hongshanornis* [Zhou & Zhang, 2005; Li et al., 2018]). The caudal ends of the ceratobranchials also seem somewhat expanded, which may suggest the presence of an epibranchial, which appears to be present in *G. zheni* BMNHC-Ph1342 and was reported in *Hongshanornis* (Zhou & Zhang, 2005; Li et al., 2018).

Comparison of the lengths of the mandible and premaxillary corpus indicate *Meemannavis* IVPP V26198 is considerably larger than IVPP V26199, *Iteravis*, and *G. zheni* (Table 1). Unlike in IVPP V26199, *Brevidentavis* V26197, *Iteravis*, and possibly IVPP V26194, the dentary of this specimen is edentulous. The dentary also is dorsoventrally shallower than that of *Iteravis* and *G. zheni*, giving it a more slender appearance (Figs. 2, 3). The dentary of *Meemannavis* IVPP V26198 steadily diminishes in dorsoventral height toward the rostral end; whereas the taper is abrupt and limited to the most rostral portion in *Brevidentavis* IVPP V26197, *Iteravis* IVPP V18958, and *G. zheni* BMNHC-Ph1342. The element tentatively identified as the maxilla of *Meemannavis* IVPP V26198 appears to resemble the maxillae of *G. zheni* BMNHC-Ph1342 and Ph1318 in possessing large, alveolus-like structures separated by thin and narrow interdental plates fused to the maxilla (Fig. 3). These putative alveoli are proportionately larger and rounder than those presumed to house the narrow, sharp maxillary teeth

preserved in IVPP V26199, which appear to be oval with a mesiodistally oriented long axis. The alveolus-like structures in the possible maxilla of *Meemannavis* IVPP V26198 are nearly twice the size of the maxillary alveoli of BMNHC-Ph1342 and Ph1318 despite the fact that the former specimen is only 25%–30% larger. It is important to note that the possible alveoli of *Meemannavis* IVPP V26198 may either be exaggerated by crushing or, potentially are preservational artifacts rather than alveoli. However, if they are indeed alveoli this would be the first identified ornithuromorph with teeth present only in the maxilla, a morphology not found elsewhere in Aves. The frontal of *Meemannavis* IVPP V26198 appears to lack the small, knob-like postorbital process present in IVPP V26194 (Fig. 6).

The frontal in IVPP V26194 bears a blunt postorbital process that appears to be absent in IVPP V26196, *Meemannavis* V26198 (as noted above), and *G. zheni* BMNHC-Ph1318. The laterally facing margin of the frontal that forms the caudodorsal portion of the orbit of IVPP V26194 and V26196 also appears absent in *G. zheni* BMNHC-Ph1318.

The most cranial eight cervical vertebrae (C1–C8) are completely preserved in IVPP V26194 and V26195, although they are dorsally exposed in IVPP V26194 and ventrally exposed in V26195 (Figs. 6, 7). As far as can be compared, the cervicals are similar between these two specimens. The atlantal rami do not appear to meet dorsally to form a continuous arch in either specimen. This plesiomorphic condition has been described in some enantiornithines, but a complete atlantal arch was reported in the Late Cretaceous ornithuromorph *Patagopteryx* (Chiappe, 2002). The vertebral proportions of both specimens are similar with the cranial cervicals being wider than long and C6 through C8 being longer than wide. The distance between C3 and C8 measures approximately 30 mm in both specimens. The orientations of the zygapophyses also are similar. One potential major

Table 1 Cranial measurements for IVPP V26194, V26195, IVPP V26196, *Brevidentavis zhangii* IVPP V26197, *Meemannavis ductrix* V26198, cf. *Gansus yumenensis* V26199, *Iteravis huchzermeyeri* V18958, and *Gansus zheni* BMNHC-Ph1342 and Ph1318

	V26194	V26195	V26196	V26197	V26198	V26199	V18958	BMNHC Ph1342	BMNHC Ph1318
Skull length						37.56	46.7*		43.87
Mandible length					45.9	31.46	38.87	36.19	37.51*
Dentary height				1.7–2.16	1.45–2.08	1.12–1.95	2.02–2.29	2.14–2.8	1.59–2.54
Dentary teeth crown height				0.416–0.47				0.825	
Dentary teeth mesiodistal length				0.48				0.34	
Predentary rostrocaudal length				1.7			1.39		1.36
Ceratobranchial length (tip to tip)				12.3		19.93			13.04
Maxilla, alveoli mesiodistal length					1.16–1.42	0.571–0.619		0.61–0.73	0.62–0.71
Premaxillary corpus (rostral tip to base of frontal process)					(10.13)	5.94*	6.53	7.09	

Measurements are in millimeters. Parentheses indicate the measurement is short either because the element is incomplete or a portion of the element is hidden from view. *Indicates an estimate.

Table 2 Vertebral measurements for IVPP V26194, V26195, V26196, *Brevidentavis zhangii* V26197, and *Meemannavis ductrix* V26198

Specimen	Vert #	Pez width	Poz width	Pez/Poz width ratio	Mid width	Pez-Poz length	Mid-arch length	Vert body length	Spine length	Spine width (Dist)
IVPP V26194 (exposed in dorsal view)	C2	4.42	6.24	0.71	3.93	5.07*	X	(5.42w/odontoid)	2.61	0.81
	C3	(4.5)	6.32	(0.71)	3.77	(4.21)	2.81	3.10	2.81	Br
	C4	4.94	6.76	0.73	4.69	(4.41)	3.64	4.59	1.40	0.35*
	C5	5.60	6.21	0.90	3.79	(5.28)	4.20	5.17	3.41*	Br
	C6	5.52	6.17	0.89	3.56	(6.50)	4.76	5.66	2.68*	0.31*
	C7	6.10	5.54	1.10	4.00	(6.65)	3.47	(5.88)	3.47	0.22*
	C8	5.54	X	X	n/a	n/a	n/a	n/a	n/a	n/a
	C8	X	5.17	X	(4.10)	X	0.31	X	X	X
IVPP V26195 (exposed in ventral view)	C3	5.83	(6.46)	(0.90)	4.05	5.28	0.50	3.28	X	X
	C4	6.08	7.27	0.84	4.41	5.63	0.33	3.41	X	X
	C5	6.38	7.35	0.87	4.61	5.75	0.63	4.47	X	X
	C6	6.60	X	X	4.18	7.41	0.69	(5.04)	X	X
	C7	6.43	6.84	0.94	4.17	7.45	0.69	5.54	X	X
	C8	X	7.21	X	4.38	7.75	0.82	5.46	X	X
	C9	7.10	X	X	X	X	X	X	3.47	X
	C3	X	3.86	X	2.93	5.96	X	4.29	X	X
	C4	X	X	X	X	6.92	X	5.22	X	X
IVPP V26196 (primarily exposed in lateral view)	C5	X	X	X	X	6.85	X	6.21	X	X
	C6	X	X	X	X	8.07	X	5.89	X	X
	C7	X	X	X	X	6.61	X	X	X	X
	C8	X	X	X	X	(5.51)	X	(5.37)	X	X
	C9	X	X	X	X	(4.67)	X	(4.73)	X	X
	Cvt1	X	X	X	X	(5.35)	X	4.86	X	X
	Cvt2	X	X	X	X	(5.92)	X	5.09	X	X
	T1	X	X	X	X	(5.4)	X	X	5.67	X
	T2	X	X	X	X	X	X	X	4.54	X
	T3	X	X	X	X	X	X	X	4.02	X
IVPP V26197 (primarily exposed in lateral view)	C2?	X	X	X	X	(4.43)	X	(3.21)	X	X
	C3?	X	X	X	X	X	X	4.65	X	X
	C4?	X	X	X	X	X	X	4.63	X	X
	C5?	X	X	X	X	X	X	(3.35)	X	X
	C6?	X	X	X	X	6.18	X	(4.03)	X	X
	C8?	X	X	X	X	6.83	X	6.06	X	X
	C9?	X	X	X	X	X	X	(5.53)	X	X
	C3?	X	X	X	X	X	X	4.86	X	X
IVPP V26198 (primarily exposed view; disarticulated)	C4?	X	X	X	X	5.57	X	X	X	X
	C5?	X	X	X	X	X	X	7.01	4.8	X
	C6?	X	X	X	X	X	X	5.16	X	X
	C7?	X	X	X	X	X	X	6.4	X	X
	T?	2.82	5.1	8.11	X	X	X	3.73	X	X

Measurements are in millimeters. Anatomical abbreviations: C, cervical; Cvt, cervicothoracic; T, thoracic; pez, prezygapophyses; poz, postzygapophyses. X = measurement unavailable in preserved view; *feature possibly broken; parentheses = incomplete or portion of element hidden from view; ? = position in vertebral sequence uncertain.

difference exists in the form of the intervertebral articulations, which are inferred to be amphicoelous or amphiplatyan in IVPP V26194, as in the caudal cervical vertebrae of *G. yumenensis*, but heterocoelous in IVPP V26195. However, the vertebrae are fully articulated, so these putative differences cannot be confirmed at present. The cervicals of IVPP V26196 and *Brevidentavis* V26197 appear proportionately more elongate than those of IVPP V26194 and V26195 (Table 2). The postaxial

cervicals of *G. zheni* are similarly elongate relative to the condition in IVPP V26194 and V26195 (Liu et al., 2014).

Comparison with described specimens of *G. yumenensis* is limited by the absence of overlapping osteological material. The most caudal cervical and all thoracic vertebrae are definitively preserved in only two *G. yumenensis* specimens: CAGS-IG-04-CM-002 and 04-CM-004 (You et al., 2006) (Fig. 2A). Only IVPP V26196, *Brevidentavis* V26197, and *Meemannavis* V26198, which preserve the most caudal

cervicals and most cranial thoracics, overlap with these *G. yumenensis* specimens. However, preservation of the vertebrae is poor in the IVPP specimens. In *Meemannavis* IVPP V26198, the most caudal cervicals and cranial thoracics are fragmented, and in *Brevidentavis* IVPP V26197, the cervicals are completely flattened. Only IVPP V26196 preserves some comparable morphology, but poor preservation limits these comparisons to the most superficial level. The most caudal three cervicals are dorsally exposed in CAGS-IG-04-CM-002 (Fig. 2A). They appear to have approximately square centra with very large and robust, caudolaterally oriented postzygapophyses; smaller, more delicate, cranio-laterally oriented prezygapophyses; and low (practically nonexistent) neural spines. In CAGS-IG-04-CM-004, the transitional cervicothoracic vertebrae are ventrally exposed, revealing pronounced, ventrally forked hypapophyses. The vertebrae forming the cervicothoracic transition of IVPP V26196 are not as elongate as the preceding cervical vertebrae. Their postzygapophyses are robust and greater in size than the prezygapophyses, the neural spines are low, and hypapophyses are present. However, they are laterally exposed and poorly preserved, preventing a more detailed comparison with *G. yumenensis*.

Given that *G. yumenensis*, *G. zheni*, and *Iteravis* share several postcranial morphological similarities and appear to be phylogenetically close to one another (Liu et al., 2014), the similarities that IVPP V26199 shares with *Iteravis* suggest, but do not definitively demonstrate, that this specimen pertains to *G. yumenensis*. IVPP V26199 shares with *Iteravis*: an edentulous, rostrally fused premaxilla with elongate, unfused frontal processes but lacking palatal processes; and the presence of numerous small, sharp teeth in the maxilla and dentary. Among Early Cretaceous birds for which the skull is known, this combination of morphologies is found only in IVPP V26199 and *Iteravis* (although rostral fusion of the premaxilla is ambiguous in IVPP V18958). However, unlike *G. zheni* BMNH-C-Ph1342, IVPP V26199 lacks epibranchials, though this may result from a lack of preservation rather than actual absence.

3.3 Cladistic analysis

All six specimens (IVPP V26194, V26195, V26196, *Brevidentavis* V26197, *Meemannavis* V26198, and V26199) were added to a modified version of the O'Connor & Zhou (2013) matrix. *Gansus zheni* BMNH-C-Ph1342 and Ph1318 also were added and scored separately from IVPP V18985, the holotype of *I. huchzermeyeri*, in order to test hypotheses that all three specimens are referable to a single taxon (Wang et al., 2018b; Ju et al., 2021). Other Changma ornithuromorphs *Changmaornis*, *Jiuquanornis*, and *Yumenornis* were also added to the dataset. The final matrix consists of 71 operational taxonomic units, 41 of which are ornithuromorphs, scored across 245 equally weighted morphological characters, 31 of which were ordered. The matrix was analyzed using TNT (Goloboff et al., 2008a) using traditional technology, conducting a heuristic search retaining the single shortest tree out of every 1000 trees followed by a second round of tree-bisection reconnection (TBR) except where we tested the impact of implied weighting by analyzing the dataset with a *k* value of 12 (Goloboff et al., 2008b). Consensus trees were obtained using both Nelsen's strict consensus and majority rule (>50%).

The first round of TBR produced a single, well-resolved tree (length 896 steps; consistency index 0.367; retention index 0.654; Fig. S2). The second round of TBR produced 10 000 trees of the same length. In the strict consensus tree, Ornithothoraces forms a massive polytomy because of the uncertain placement of *Chaoyangia*. Removal of this taxon in a reduced strict consensus tree results in resolution between Enantiornithes and Ornithuromorpha (Fig. S3). However, all ornithuromorphs more derived than *Archaeorhynchus* form a large polytomy, at least partially reflecting the fragmentary nature of several of the specimens included in the analysis (e.g., only three characters could be scored for V26196 and V26194). The majority rule (>50%) consensus tree produces a well resolved Ornithuromorpha (Fig. 9A). We conducted an analysis using implied weighting (*k* value set at 12) and it produced a single well-resolved tree (Fig. 9B).

In both the majority rule tree and the tree produced using implied weighting, IVPP V26195, V26196, IVPP V26199, *Meemannavis* IVPP V26198, and *Brevidentavis* IVPP V26197 are confirmed as ornithuromorphs. In both analyses, IVPP V26194 (only three characters scored; 98.8% missing data) was found to be a basal non-pygostylian bird, in a polytomy with *Jeholornis* outside Pygostylia in the majority rule tree but stemward of *Jeholornis* in the implied weighting analysis (Fig. 9). Both analyses resolve Confuciusornithiformes and *Sapeornis* as the successive outgroup to Ornithothoraces. The two trees differ in the relative placement of taxa within the two ornithothoracine clades, particularly with regards to Ornithuromorpha, although some relationships are consistent or very similar between both phylogenetic hypotheses. Within Enantiornithes, *Eoenantiornis*, a clade consisting of *Neuquenornis* + *Otogornis* + *Vescornis* + *Gobipteryx* (precise relationships differ), Pengornithidae, *Elsornis*, and *Protopteryx* form successive outgroups with *Protopteryx* resolved in the most basal position. Longipterygidae is resolved in a derived position with *Eocathayornis* as its outgroup. *Iberomesornis* is placed within the Longipterygidae as sister taxon to the Longipteryginae in the implied weighting analysis, but in a polytomy with Longirostravinae and Longipteryginae in the majority rule tree. The two *G. zheni* specimens form a clade supporting their referral to a single specimen (the one scoring that differs between the two specimens, character 165, relates to distal fusion of the metacarpals and most likely reflects differences in relative ontogenetic stage). *Brevidentavis* is resolved within the Hesperornithiformes. *Ichthyornis* is recovered as the sister taxon to Neornithes, in which *Gallus* is resolved as the sister taxon to *Vegavis* (Fig. 9).

In the majority rule tree, Hesperornithiformes consists of *Brodavis* and *Baptornis* forming successive outgroups to a *Parahesperornis* + *Hesperornis* clade, with *Enaliornis* and *Brevidentavis* in a basal polytomy. Hesperornithiformes forms a dichotomy with the *Ichthyornis* + Neornithes clade. *Changmaornis* forms the outgroup to this dichotomy. *Iteravis*, *Jiuquanornis*, and *G. zheni* form a polytomy with the clade formed by *Changmaornis* + crownward ornithuromorphs. This clade forms a dichotomy with a clade consisting of *Patagopteryx* + *Longicrusavis* with *Apsaravis* and *Hongshanornis* as successive outgroups. IVPP V26196, *Limenavis* + *G. yumenensis* + *Yumenornis*, and a clade consisting of *Hollandia* + *Songlingornis* + *Archaeornithura* with *Yanornis* and



Fig. 9. Cladogram depicting the hypothetical relationships of the Xiagou ornithuromorph skulls relative to other Mesozoic bird taxa. **A**, Majority rule (>50) tree produced from 10 000 trees with lengths of 896 steps produced following two rounds of tree bisection reconnection (the first round produced a single well resolved tree of the same length with a consistency index of 0.367 and a retention index of 0.654) – values indicate the percentage of trees in which each node is resolved. **B**, The single tree (consistency index = 0.367; retention index = 0.654) produced when implied weighting was applied ($k = 12$).

Yixianornis as successive outgroups, form a polytomy with all crownward taxa. *IVPP V26199* and *Ambiortus* form successive outgroups to this polytomy. *Meemannavis*, *Dingavis*, *Jianchangornis*, *Chaoyangia*, and a clade formed by a polytomy between *Zhongjianornis* + *Xinghaiornis*, *Schizooura* and *IVPP V26195* form a polytomy with all more derived ornithu-

romorphs. *Archaeorhynchus* is resolved as the most basal ornithuromorph (Fig. 9A).

In the tree produced using implied weighting, Hesperornithiformes consists of *Hesperornis*, *Brodavis*, *Baptornis*, and *Enaliornis* forming successive outgroups to *Parahesperornis* + *Brevidentavis*. Hesperornithiformes forms a

dichotomy with the clade consisting of *Ichthyornis* and *Limenavis* forming successive outgroups to Neornithes. *Changmaornis*, *Ambiortus* + *Apsaravis*, *Jiuquanornis*, and a clade formed by *Yumenornis* as outgroup to *G. yumenensis* + IVPP V26199 form successive outgroups to the dichotomy between Hesperornithiformes and crownward taxa. A clade consisting of *Archaeornithura* + *Hollanda* with *Songlingornis*, *Yanornis*, and *Yixianornis* forming successive outgroups forms the outgroup to crownward taxa. This inclusive clade forms a dichotomy with a clade consisting of *G. zheni* + *Iteravis* in a dichotomy with *Hongshanornis* + *Longicrusavis*. *Dingavis*, *Jianchangornis*, and *Meemannavis* form successive outgroups to all crownward taxa. The *Meemannavis* + all more derived ornithuromorphs clade forms a dichotomy with a clade formed by *Xinghaiornis* + IVPP V26195 with *Zhongjianornis* and *Schizooura* as successive outgroups. A clade consisting of *Patagopteryx* as the outgroup to *Archaeorhynchus* + IVPP V26196 forms a dichotomy with all more derived taxa. *Chaoyangia* is resolved as the most basal ornithuromorph (Fig. 9B).

4 Discussion

Outside of the deposits in northeastern China that record the Jehol Biota, the Xiagou Formation is the only other geologic unit in China to produce Early Cretaceous avian remains. Thus the avian assemblage from the Xiagou Formation is important for broadening the extent of our knowledge of avifaunas in terms of diversity and geographic distribution during this important time in bird evolution. The Changma locality has produced a handful of ornithothoracine taxa that together reveal important aspects of early avian biology such as complex tail plumage, medullary bone, and eggshell microstructure (O'Connor et al., 2016b; Bailleul et al., 2019b). Although dozens of bird fossils have been recovered (You et al., 2006; Li et al., 2011; Wang et al., 2016c), the six skull-bearing specimens described here constitute the first avian cranial remains reported from the Xiagou Formation. Descriptions of these specimens are therefore important for clarifying the ecological and morphological diversity of ornithuromorph birds in the Xiagou paleoecosystem.

4.1 Taxonomic diversity in the Changma avifauna

Unfortunately, a precise understanding of this diversity is hindered by differences in which bones are present in each specimen, how they are exposed, and their qualities of preservation. Among previously recognized ornithuromorphs from the Xiagou Formation, only *G. yumenensis*, the taxon most commonly recovered from the Changma locality (see Section 4.3), preserves material that can be directly compared to these new specimens. This situation, however, is limited to the most caudal cervicals, which are preserved in only two specimens of *G. yumenensis* (CAGS-IG-04-CM-002 and 04-CM-004) and three of the specimens reported here (IVPP V26196, *Brevidentavis* V26197, and *Meemannavis* V26198), and the most cranial thoracic vertebrae, which are preserved in five specimens of *G. yumenensis* (CAGS-IG-04-CM-002, 04-CM-003, and 04-CM-004, and GSGM-07-CM-009 and 07-CM-011), and three of the specimens reported here (IVPP V26196, *Brevidentavis* V26197, and *Meemannavis*

V26198). Three of the specimens described here (IVPP V26194, V26195, and V26199) have no osteological overlap with previously reported avian specimens from the Changma locality. While preservation of the most caudal cervicals is excellent and three-dimensional in *G. yumenensis* CAGS-IG-04-CM-002 and 04-CM-004, the comparable vertebrae are poorly preserved and crushed in IVPP V26196, *Brevidentavis* V26197, and *Meemannavis* V26198. As such, assignment of any of the new material to *G. yumenensis* based on direct comparison is problematic at best, particularly because no clearly diagnostic characters of the cervical vertebrae have yet been identified in this taxon.

Despite the challenges associated with comparing the material, at least three ornithuromorph taxa are represented among the six specimens preserving skull material. *Brevidentavis* IVPP V26197, *Meemannavis* V26198, and V26199 each pertain to different taxa based on differences in the dentary dentition: the dentary teeth are brachydont and blunt in *Brevidentavis* IVPP V26197 (Fig. 4); slender, closely spaced, and sharp in IVPP V26199 (Fig. 5); and absent altogether in *Meemannavis* IVPP V26198 (Fig. 3). *Brevidentavis* IVPP V26197 can be further distinguished by having its teeth arranged in a communal groove rather than in distinct sockets, a condition also exhibited in *Hesperornis* (Dumont et al., 2016). *Meemannavis* IVPP V26198 is also considerably larger than the other specimens, which might be a diagnostic feature of this largely or wholly edentulous taxon (Table 1).

Differences among IVPP V26199, *Brevidentavis* V26197, and *Meemannavis* V26198 justify the erection of new taxa for the latter two specimens, for which we erect the respective taxonomic names, *Brevidentavis zhangi* and *Meemmanavis ductrix* gen. et sp. nov. Three other named ornithuromorph taxa (*Jiuquanornis*, *Changmaornis*, and *Yumenornis*), only two of which preserve material that overlaps with the other, have been described from the Xiagou Formation on the basis of postcranial remains (Wang et al., 2013). Though the two new taxa erected herein could conceivably be junior synonyms of any of them, this is presently impossible to determine because of a lack of directly comparable fossils. Given the currently available material is distinct from all known Early Cretaceous birds, we choose to erect new taxa, which can be synonymized should new material prove that to be necessary. Similarly, the taxonomic diversity of the Xiagou avifauna may be slightly overestimated in the current literature because *Changmaornis* cannot be directly compared to *Jiuquanornis* or *Yumenornis*. Therefore, the former taxon could be a synonym of one of the latter two. However, the discovery of three distinct cranial morphologies confirms that the Xiagou avifauna had a diverse ornithuromorph component that lived alongside several enantiornithine birds, similar to the Jehol avifauna. The dental diversity, along with other cranial features described above, also implies these birds differed substantially in their foraging strategies and diets. Nevertheless, without additional, directly associated postcranial material, we cannot hypothesize what aspects of the local paleoecosystem they occupied and exploited.

In addition, IVPP V26194 and V26195 can be distinguished from IVPP V26196 and *Brevidentavis* V26197 based on the proportions of their cervical vertebrae (Table 2). IVPP V26194 is resolved in our phylogenetic analysis in a very basal

position, closely aligned to the long-bony-tailed bird *Jeholornis* (Fig. 9). This relationship is not supported by our morphological observations; for example, both the elongate morphology of the frontal processes of the premaxilla and the presence of a postorbital process on the frontal are more consistent with identification of this specimen as an ornithuromorph. We attribute the basal position resolved for this specimen to the limited number of morphological characters that could be confidently scored into the current matrix and continue to regard the known Xiagou Formation avifauna as consisting entirely of ornithothoracines.

The Jehol ornithuromorphs *Iteravis huchzermeyeri* and *G. zheni* from the relatively recently discovered Sihedang locality, both known from several complete skeletons (Liu et al., 2014; Zhou et al., 2014; Chiappe & Meng, 2016; Wang et al., 2018b), are considered to be synonymous by some (Wang et al., 2018b; Ju et al., 2021). The two taxa are resolved forming a single clade in the implied weighting analysis with *Iteravis* differentiated from *G. zheni* because it lacks a cranial projection of the sternolateral process on the coracoid (character 95), a feature notably present in *G. yumenensis* (You et al., 2006). However, this region of the coracoid is poorly preserved in *Iteravis* IVPP V18958, and this delicate process may have been damaged post-mortem. Alternatively, Ju et al. (2021) hypothesize the absence of this cranial projection is ontogenetic. We concur with previous studies that *G. zheni* is most likely a junior synonym of *I. huchzermeyeri* (Ju et al., 2021). However, pending a detailed study of all referred specimens, the question of synonymy remains inconclusive, and we refer to these taxa separately but as representing a grade, reflecting their very close (if not synonymous) relationship.

Previous analyses have recovered *Iteravis* in a phylogenetically close relationship to *G. yumenensis* based on postcranial morphology (Liu et al., 2014; Wang et al., 2018b), with *G. zheni* recovered as forming a clade with *G. yumenensis* in a previous analysis (Liu et al., 2014). A close relationship between *G. zheni/Iteravis* and *G. yumenensis* is not supported in the analyses presented here. However, relationships among the ornithuromorphs in our analysis are very weakly supported, forming a large polytomy in the strict consensus tree created without using implied weighting. The close relationship among *G. yumenensis*, *Iteravis*, and *G. zheni* resolved in previous phylogenetic analyses is supported by clear morphological similarities in the postcrania (e.g., sternolateral process of the coracoid as described above, as well as similarities in the sternum, foot, and other body parts) (Wang et al., 2018b) although important differences between these taxa are noted by Ju et al. (2021) (e.g., differences in coracoid symmetry).

IVPP V26199, the most complete Xiagou skull (and the only skull to preserve most of the rostrum) cannot be compared directly to any specimen of *G. yumenensis* because it only preserves the most cranial cervical vertebrae. However, comparison to skulls preserved in several specimens of *Iteravis* and *G. zheni* (Liu et al., 2014; Zhou et al., 2014; Wang et al., 2018b) suggests that IVPP V26199 may be referable to *G. yumenensis*, and that the morphological similarity between these taxa extends to the cranium. Comparisons are limited because IVPP V26199 is primarily exposed in ventral view, and all specimens of *Iteravis* and *G. zheni* preserve the skull

primarily in lateral view. In both IVPP V26199 and *Iteravis*, the premaxillae are edentulous and lack palatal processes. In addition, the maxillae and dentaries of *Iteravis* and *G. zheni* are fully toothed, bearing numerous, closely spaced, delicate, and sharply pointed teeth (Fig. 2B), and the toothed rostral end of the dentary would have occluded with the edentulous premaxilla. A predentary bone, preserved in *Iteravis* IVPP V19858 and *G. zheni* BMNH-Ph1342, is not preserved in IVPP V26199, but the dentary bears a rostralateral foramen through which the facial nerve probably innervated the missing predentary (Bailleul et al., 2019a).

Given the numerical dominance of specimens of *G. yumenensis* in the Xiagou Formation, the statistical likelihood of at least one of the six skull specimens being referable to this taxon is very high. Therefore, based on the similarities between IVPP V26199 and *Iteravis*, we tentatively refer this specimen to *G. yumenensis*, a hypothesis supported by the implied weighting analysis (Fig. 9B). Although we do not refer IVPP V26194 and V26195 to any specific taxon at this time, we suggest that, in the future, new data may reveal that these two specimens are also referable to *G. yumenensis*. These two specimens, where limited comparison is possible, are consistent with each other (similar proportions of the cervical vertebrae, atlantal arches unfused), and their referral to *G. yumenensis* would be consistent with the proportions of taxa recovered from the Changma locality (see Section 4.3). Unfortunately, the limited number of characters that can be scored at this time for these fragmentary specimens prevents accurate assessment of their phylogenetic position through cladistic analysis. Despite its odd position in our phylogenetic analyses, IVPP V26194, like IVPP V26199, has elongate frontal processes of the premaxilla, conical dentary teeth, a bowed jugal, and it appears to have a supraorbital salt gland shared with *Iteravis/G. zheni* (Wang et al., 2018b) (Fig. 6).

4.2 Aulacodony in Aves

Interdental plates are not visible separating the dentary teeth in *Brevidentavis* IVPP V26197 and CT images support the interpretation that interdental bone was absent in this specimen such that the teeth are arranged in a communal groove. This morphology, referred to as aulacodony, has otherwise only been reported within Aves in some crownward ornithurines: *Hesperornis* (Gregory, 1952) and immature specimens of *Ichthyornis* (Martin & Stewart, 1977). In contrast, *Archaeopteryx* possesses the typical “thecondont” condition (Martin & Stewart, 1999) in which teeth are separated by interdental bone (used *sensu* [LeBlanc et al., 2017]), and thus each tooth is supported by bony walls on four sides (Bertin et al., 2018). Subsequent discoveries have confirmed that thecodonty is the typical condition present in most toothed birds. Interdental bone is present in non-ornithothoracines (e.g., *Sapeornis*) (Wang et al., 2017b), enantiornithines (clearly visible in *Pengornis*) (Zhou et al., 2008; O'Connor & Chiappe, 2011), and at least some non-ornithurine ornithuromorphs (visible in published CT data of *Yanornis* and *Similiyanornis*) (Bailleul et al., 2019a; Wang et al., 2020b). Though interdental bone accumulates through ontogeny, as observed in extant crocodylians and *Ichthyornis* (LeBlanc et al., 2017), there is no evidence that IVPP V26197 might be somatically immature.

Tooth implantation in the dentary of IVPP V26199 is not clearly discernible because of differences in the CT scanner used to image this specimen compared to the industrial CT scanner used for *Brevidentavis* IVPP V26197. The differences in the scanners used are related to fossil specimen slab sizes. Interdental bone also may be absent in IVPP V26199, but pending the possibility of collecting higher resolution digital data in the future, interpretations for this specimen are equivocal. Along with *Brevidentavis* IVPP V26197, *Iteravis* IVPP V18958 also was scanned using the industrial CT scanner as part of a previous study on the avian predentary (Bailleul et al., 2019a). In the scans of *Iteravis* IVPP V18958, several details can be discerned: a resorption pit is visible in the first dentary tooth; the third tooth appears to be still growing; and interdental bone is not visible. In some areas, the teeth are not *in situ*, having been rotated distally. This condition also occurs in *Hesperornis* and is inferred to be the result of the absence of interdental bone holding the teeth in place mesiodistally (Dumont et al., 2016). In contrast, in the scans of *Yanornis* IVPP V13358 (Bailleul et al., 2019a), narrow strips of interdental bone are visible clearly between the dentary teeth, along with other features such as the presence of resorption pits for replacement teeth (Bailleul et al., 2019a: figs. 1c–1e).

In *Hesperornis*, both the maxillary and dentary teeth are aulacodont (Marsh, 1880). However in *G. zheni* BMNH-Ph1342, the maxillary teeth are clearly separated by narrow septa of interdental bone (Chiappe & Meng, 2016), and similarly narrow septa appear present in the maxilla of IVPP V26199. Since the interdental bone in both specimens is very narrow, such delicate structures may have been lost because of postmortem damage to the dentary of *Iteravis* IVPP V18958. At this time, among Early Cretaceous birds, aulacodonty can be determined unequivocally only to be present in *Brevidentavis* IVPP V26197 with available data.

The loss of interdental bone most likely evolved multiple times in Aves (e.g., possibly independently in *Brevidentavis* IVPP V26197 and hesperornithiforms) (Dumont et al., 2016) as in non-avian theropods. Interdental plates are absent in the ornithomimosaur *Pelecanimimus* (Pérez-Moreno et al., 1994), the dromaeosaurid *Buitreraptor* (Gianechini et al., 2017), and in the rostral portions of the dentaries in some troodontid theropods (Currie, 1987). In the latter, the loss of interdental plates has been attributed to the presence of numerous, tightly spaced teeth (Currie, 1987). *Pelecanimimus* similarly has numerous, tightly spaced teeth, more than any other theropod (Pérez-Moreno et al., 1994). This situation also may explain the absence of interdental bone in *Brevidentavis* IVPP V26197 and possibly *Iteravis*, in which the teeth are similarly closely spaced. Alternatively, the absence of interdental bone may be a synapomorphy of the clade that includes IVPP V26197 and Hesperornithiformes, as resolved by our cladistic analysis (Fig. 9). Although the results of our cladistic analyses resolve *Brevidentavis* IVPP V26197 as a hesperornithiform, this relationship in the majority rule tree is based entirely on the single character state describing the dentary teeth in a communal groove (35:1) with all other supporting character data, mostly pertaining the hindlimb, scored as missing data for *Brevidentavis* IVPP V26197. Tooth morphology is significantly different between *Brevidentavis* IVPP V26197 and hesperornithiforms, which also suggests ecological differ-

ences that further do not support a close phylogenetic relationship between these two taxa. The high-crowned, carinated, curved, and laterally compressed morphology of the teeth in hesperornithiforms are interpreted as adapted for piscivory, consistent with the foot-propelled aquatic hindlimb morphology that characterizes this group. It is unclear for what function the blunt teeth in *Brevidentavis* IVPP V26197 evolved, and without non-axial postcranial remains for this taxon, there is very little evidence with which to hypothesize its ecological habits. Given the differences in dental and dentary morphology and the absence of any postcranial remains that could further support this placement, we do not consider *Brevidentavis* IVPP V26197 to be a hesperornithiform at this time.

4.3 Relative abundance

The majority of the dozens of avian specimens recovered from the Changma locality are referred to *G. yumenensis*. Out of 40 previously reported specimens, only 12 have been identified as referable to taxa other than *G. yumenensis* (i.e., 70% are referable to *G. yumenensis*), nine of which have been referred to the Enantiornithes (You et al., 2005, 2006, 2010; Harris et al., 2006; Ji et al., 2011; Li et al., 2011; O'Connor et al., 2012, 2016b; Nudds et al., 2013; Wang et al., 2013, 2016b, 2016c; Bailleul et al., 2019b). Thus, it is somewhat surprising that out of six skull specimens described here, three separate taxa can be identified, and a fourth specimen (IVPP V26196) is determined at least to not pertain to *G. yumenensis* (although preservation is too poor to justify placing it in a new species). In other words, 50% of the cranial specimens definitively are not referable to *G. yumenensis*. This situation may suggest that some postcranial specimens previously identified as *G. yumenensis* in fact are not referable to this taxon. However, that idea seems plausible only for the most fragmentary described specimens such as those consisting of partial forelimbs (i.e., GSGM-07-CM-006).

The fact that all of the skulls are referable to the Ornithuromorpha is unsurprising. Although over one-fifth of the Changma bird specimens described thus far are enantiornithines, this diversity does not reflect their true proportion of specimens recovered from the Xiagou Formation avifauna. Numerous ornithuromorph specimens, mostly presumed to be referable to *G. yumenensis*, have been collected that are as yet undescribed given their fragmentary nature, with some consisting of only isolated elements. Currently, only the most complete specimens and those representing new diversity have been reported, representing less than half of the total recovered specimens.

Comparison with specimens from Jehol localities is limited because of differences in collection (a majority of Jehol specimens collected by non-paleontologists) and publication (published Jehol specimens dominated by holotypes) biases that result in a greater amount of exceptional material made available from the Jehol localities. Accurate total numbers of specimens collected are not available for any locality in the Jehol and even locality information itself is often imprecise and or only tentative. However, while only three enantiornithine specimens have been described from Sihedang (Hu & O'Connor, 2017; Wang et al., 2020a; Wang & Zhou, 2020), ten ornithuromorph specimens have been described, eight of

which are *Iteravis-G. zheni* grade (four specimens of *Iteravis* and four of *G. zheni*) (Liu et al., 2014; Zhou et al., 2014; Chiappe & Meng, 2016; Wang et al., 2018b). In addition, the Sihedang locality has produced one specimen of *Sapeornis chaoyangensis* (Hu et al., 2020) and one confuciusornithiform – *Yangavis confucii* – a unique taxon known from a single specimen (Wang & Zhou, 2018). Although the degree of dominance by a single ornithuromorph taxon has diminished as more specimens are published from the Sihedang locality, *Iteravis/G. zheni* account for eight of the 15 published bird specimens (53%). Furthermore, numerous *Iteravis/G. zheni* specimens have yet to be published because publication has again focused on new diversity. In contrast, all other taxa are known from single specimens, with the possible exception of *Dingavis longimaxilla* and *Changzuornis ahgmi*, which may be synonymous (Huang et al., 2016; O'Connor et al., 2016a).

4.4 Taphonomy of the Changma locality

The taphonomy of the Changma locality of the Xiagou Formation appears distinct from that of the Jehol Group including that specific to the Sihedang locality that has similarly produced an ornithuromorph dominant avifauna. In the first description of a bird from Sihedang, the similar dominance of ornithuromorphs at both the Sihedang and Changma localities was suggested to possibly indicate a unique, aquatic paleoenvironment recorded at both localities (Zhou et al., 2014). However, notable differences exist between the recorded fauna, preservation, and sedimentology at each locality that weaken this original hypothesis.

Although both deposits are largely lacustrine in origin, very few fish fossils were recovered from Changma during the expeditions in 2004–2008, in contrast to the thousands of fish recovered from Jehol deposits (Chang et al., 2003). This may be the result of the absence of volcanic influence in the Xiagou Formation, which produced mass mortality events during the deposition of the Jehol Biota (Wang & Zhou, 2003). Unfortunately, no information is available pertaining to fish fossils from the Sihedang locality, although the cooccurrence of more than one complete specimen of *Iteravis/G. zheni*-grade ornithuromorph preserved in close association on a single slab provide evidence of mass mortality events typical of Jehol deposits (e.g., AGB5834-1/2, BMNHC-Pho01392) (Chiappe & Meng, 2016; Wang et al., 2018b). The Changma fauna also differs noticeably in the absence of non-ornithothoracine birds and pterosaurs, both of which have been recovered at Sihedang. The pterosaur fauna from Sihedang is quite diverse and records species also found at other localities (Wang et al., 2014; Lü et al., 2016a, 2016b; Zhang et al., 2019). Similarly, some birds found at Sihedang have been collected from other localities. For example, the enantiornithine *Piscivorenantionis* is known from Dapingfang (Wang et al., 2016a) and *Juehuaornis*, a possible synonym of *Dingavis/Changzuornis*, comes from the Sanjiazhi locality (Wang et al., 2015b).

In contrast to avian specimens from the Jehol Biota, the Changma specimens do not react under laser-stimulated fluorescence, but this absence of reactivity may result from the thick layer of consolidant applied to the Changma specimens. In addition, CT scans commonly reveal regions of unusually high density in the skeletons of Changma specimens (Fig. 3). Such regions probably indicate the deposition

of minerals such as pyrite that are not uncommon in fossils. However, the presence of such high-density mineral deposits visible in CT scans is more common in Changma fossils than it is in those from the Jehol. This contrasting preservation may result from higher ion concentrations in the Changma paleolake relating to seasonal dryness (Suarez et al., 2017).

Compaction in the Xiagou Formation sediments also appears to have been less than that experienced by the Jehol Group deposits because most specimens recovered from Changma retain some degree of their original three-dimensional morphology; whereas this type of preservation in the Jehol is very rare (You et al., 2006). In fact, such three-dimensional preservation, when reported in Jehol specimens (including one from Sihedang), is usually the result of the preservation of medullary bone (O'Connor et al., 2018; Wang et al., 2020a). Differences in compaction also are reflected in the fact that the Changma sediments are more poorly indurated, being softer than the mudstones that form the Jehol deposits. The Changma sediments also are darker in color, which likely reflects a high amount of organic carbon (Suarez et al., 2017). These observations indicate major differences between the geochemistry and taphonomic histories of the Changma locality and Jehol deposits.

Of the avian specimens reported from Sihedang, a majority (including all known specimens of *Iteravis* and *G. zheni*) are complete and fully articulated (corresponding to taphonomic Stages 1 and 2 of Davis & Briggs, 1998). Three exceptions have been published: the referred specimen of *Piscivorenantionis*, which like the holotype (reportedly not from Sihedang), is nearly complete but completely disarticulated; the holotype of *Mirusavis parvus*, which preserves approximately one-third of the skeleton with bones fully articulated (Wang et al., 2020a; Wang & Zhou, 2020); and *Sapeornis* IVPP V19508 which is partially disarticulated but largely complete (Hu et al., 2020) and thus somewhat intermediate in its preservation between the complete and articulated *Iteravis/G. zheni* specimens and the preservation in *Piscivorenantionis* IVPP V22362.

In contrast, no complete avian specimen has yet been recovered from the Xiagou Formation. Most Changma specimens still retain a certain degree of articulation (corresponding to Stage 3 of Davis & Briggs, 1998) including those skulls with parts of the articulated cervical columns, but individual, isolated elements also have been recovered (Stage 5, Davis & Briggs, 1998). This variation suggests a greater degree of postmortem decay and/or transport (and therefore, presumably, time) prior to burial (Davis & Briggs, 1998) within the depositional environment of the Xiagou Formation recorded at the Changma locality relative to that experienced by specimens from the Jehol Group. Differences in relative completeness among specimens may indicate differences in the impacts of factors such as water currents and, possibly, scavenging, that transported and dispersed disarticulated parts of the skeleton. Davis and Briggs (1998) noted that the skull is frequently the first element to separate from the body (Stage 3a), and sometimes remains attached to cervical vertebrae, but more often completely detaches. However, all skulls recovered from the Changma locality remain attached to at least some of their cervical vertebrae. Differences in the pattern of post-mortem disarticulation between Cretaceous

birds and modern observations may reflect aspects of the primitive anatomy of stem birds.

5 Conclusions

We describe six specimens of ornithuromorph birds consisting of skull remains preserved together with presacral axial vertebrae. Phylogenetic analyses support our identification of these as members of Ornithuromorpha except for one specimen (which in the matrix has 98.8% missing data). The six specimens represent at least three different specific taxa. The dentary dentition clearly distinguishes among three specimens. We erect new taxa for two specimens: *Brevidentavis zhangi*, characterized by low-crowned, closely spaced dentary teeth in a communal groove (the latter feature likely evolved convergently with hesperornithiforms); and *Meemannavis ductrix*, in which the dentary is edentulous. One specimen is referred tentatively to *Ganus yumenensis* based on indirect comparisons with *Iteravis* and *Ganus zheni*. We also suggest two fragmentary specimens may later prove to be referable to *G. yumenensis*, which dominates the Changma avifauna numerically. The underlying cause of the ornithuromorph dominance at the Changma locality, and similarly at the Sihedang locality in northeastern China, remains unknown.

Acknowledgements

This research was supported by the National Natural Science Foundation of China (Grant No. 41688103) and the Strategic Priority Research Program of the Chinese Academy of Sciences (Grant No. XDB26000000). Thomas A. Stidham is supported by the National Natural Science Foundation of China (Grant No. 41772013). Alida M. Bailleul also thanks the Chinese Academy of Sciences-Presidential International Fellowship Initiative Program. We thank Wei Gao (IVPP) for photographing the specimens, Andrew McAfee (Carnegie Museum of Natural History) for producing Figs. 1 and 9, and Ben Creisler for etymological advice. All authors contributed to analysis of the new specimens and writing the manuscript.

References

- Bailleul AM, Li Z-H, O'Connor JK, Zhou Z-H. 2019a. Origin of the avian predentary and evidence of a unique form of cranial kinesis in Cretaceous ornithuromorphs. *Proceedings of the National Academy of Sciences USA* 116: 24696–24706.
- Bailleul AM, O'Connor J, Zhang S-K, Li Z-H, Wang Q, Lamanna M, Zhu X-F, Zhou Z-H. 2019b. An Early Cretaceous enantiornithine (Aves) preserving an unlaidd egg and probable medullary bone. *Nature Communications* 10: 1–10.
- Baumel JJ, Witmer LM. 1993. Osteologia. In: Baumel JJ, King AS, Breazile JE, Evans HE, Vanden Berge JC eds. *Handbook of avian anatomy: Nomina anatomica avium*. second edition. Cambridge: Nuttall Ornithological Club. 45–132.
- Bell A, Chiappe LM. 2020. Anatomy of *Parahesperornis*: Evolutionary mosaicism in the Cretaceous Hesperornithiformes (Aves). *Life* 10: 1–108.
- Bertin TJ, Thivichon-Prince B, LeBlanc AR, Caldwell MW, Viriot L. 2018. Current perspectives on tooth implantation, attachment, and replacement in amniota. *Frontiers in Physiology* 9: 1–20.
- Brinkman DB, Yuan C-X, Ji Q, Li D-Q, You H-L. 2013. A new turtle from the Xiagou Formation (Early Cretaceous) of Changma Basin, Gansu Province, PR China. *Palaeobiodiversity and Palaeoenvironments* 93: 367–382.
- Chang M-M, Chen P-J, Wang Y-Q, Wang Y, Miao D-S eds. 2003. *The Jehol fossils: The emergence of feathered dinosaurs, beaked birds and flowering plants*. Shanghai: Shanghai Scientific & Technical Publishers.
- Chiappe LM. 1999. *Mesozoic birds*. Embryonic Encyclopedia of Life Sciences: Nature Publishing Group.
- Chiappe LM. 2002. Osteology of the flightless *Patagopteryx deferrariisi* from the late Cretaceous of Patagonia (Argentina). In: Chiappe LM, Witmer LM eds. *Mesozoic birds: Above the heads of dinosaurs*. Berkeley, CA: University of California Press. 281–316.
- Chiappe LM, Ji S, Ji Q, Norell MA. 1999. Anatomy and systematics of the Confuciusornithidae (Theropoda: Aves) from the late Mesozoic of northeastern China. *Bulletin of the American Museum of Natural History* 242: 1–89.
- Chiappe LM, Meng Q-J. 2016. *Birds of stone*. Baltimore, MD, United States: John Hopkins University Press.
- Chiappe LM, Zhao B, O'Connor JK, Gao C-H, Wang X-R, Habib M, Marugan-Lobon J, Meng Q-J, Cheng X-D. 2014. A new specimen of the Early Cretaceous bird *Hongshanornis longicresta*: Insights into the aerodynamics and diet of a basal ornithuromorph. *PeerJournal* 2: 1–28.
- Clarke JA. 2004. Morphology, phylogenetic taxonomy, and systematics of *Ichthyornis* and *Apatornis* (Avialae: Ornithurae). *Bulletin of the American Museum of Natural History* 286: 1–179.
- Currie PJ. 1987. Bird-like characteristics of the jaws and teeth of troodontid theropods (Dinosauria, Saurischia). *Journal of Vertebrate Paleontology* 7: 72–81.
- Davis PG, Briggs DEG. 1998. The impact of decay and disarticulation on the preservation of fossil birds. *Palaios* 13: 3–13.
- Dumont M, Tafforeau P, Bertin T, Bhullar B-A, Field DJ, Schulp A, Strilisky B, Thivichon-Prince B, Viriot L, Louchart A. 2016. Synchrotron imaging of dentition provides insights into the biology of *Hesperornis* and *Ichthyornis*, the “last” toothed birds. *BMC Evolutionary Biology* 16: 1–28.
- Elzanowski A. 1991. New observations on the skull of *Hesperornis* with reconstruction of the bony palate and otic region. *Postilla* 207: 1–20.
- Elzanowski A, Wellnhofer P. 1996. Cranial morphology of *Archaeopteryx*: evidence from the seventh skeleton. *Journal of Vertebrate Paleontology* 16: 81–94.
- Field DJ, Hanson M, Burnham DA, Wilson LE, Super K, Ehret D, Ebersole JA, Bhullar B-A. 2018. Complete *Ichthyornis* skull illuminates mosaic assembly of the avian head. *Nature* 557: 96.
- Gianechini FA, Makovicky PJ, Apesteguía S. 2017. The cranial osteology of *Buitreraptor gonzalezorum* Makovicky, Apesteguía, and Agnólin, 2005 (Theropoda, Dromaeosauridae), from the late Cretaceous of Patagonia, Argentina. *Journal of Vertebrate Paleontology* 37: e1255639.
- Goloboff PA, Farris JS, Nixon KC. 2008a. TNT, a free program for phylogenetic analysis. *Cladistics* 24: 774–786.
- Goloboff PA, Carpenter JM, Arias JS, Esquivel DRM. 2008b. Weighting against homoplasy improves phylogenetic analysis of morphological data sets. *Cladistics* 24: 1–16.

- Gregory JT. 1952. The jaws of the Cretaceous toothed birds, *Ichthyornis* and *Hesperornis*. *Condor* 54: 73–88.
- Harris JD, Lamanna M, Li D, You H-L. 2009. Avian cranial material and cranial cervical vertebrae from the lower Cretaceous Xiagou Formation of Gansu Province, China. *Journal of Vertebrate Paleontology* 29: 111A.
- Harris JD, Lamanna MC, You H-L, Ji S-A, Ji Q. 2006. A second enantiornithean (Aves: Ornithothoraces) wing from the Early Cretaceous Xiagou Formation near Changma, Gansu Province, People's Republic of China. *Canadian Journal of Earth Sciences* 43: 547–554.
- Hou L, Liu Z. 1984. A new fossil bird from lower Cretaceous of Gansu and early evolution of birds. *Scientia Sinica, Series B* 27: 1296–1301.
- Hu H, O'Connor JK. 2017. First species of enantiornithes from Sihedang elucidates skeletal development in Early Cretaceous enantiornithines. *Journal of Systematic Palaeontology* 15: 909–926.
- Hu H, O'Connor JK, McDonald PG, Wroe S. 2020. Cranial osteology of the Early Cretaceous *Sapeornis chaoyangensis* (Aves: Pygostylia). *Cretaceous Research* 113: 1–13.
- Huang J-D, Wang X, Hu Y-C, Liu J, Peteya JA, Clarke JA. 2016. A new ornithurine from the Early Cretaceous of China sheds light on the evolution of early ecological and cranial diversity in birds. *PeerJournal*. 4: 1–22.
- Jehl JR, Jr. 2017. Feather-eating in grebes: A 500-year conundrum. *The Wilson Journal of Ornithology* 129: 446–458.
- Ji S-A, Atterholt JA, O'Connor JK, Lamanna M, Harris J, Li D-Q, You H-L, Dodson P. 2011. A new, three-dimensionally preserved enantiornithian (Aves: Ornithothoraces) from Gansu Province, northwestern China. *Zoological Journal of the Linnean Society* 162: 201–219.
- Ji S-A, Ji Q, You H-L, Lü J-C, Yuan C-X. 2006. Webbed foot of an Early Cretaceous ornithurine bird *Gansus* from China. *Geological Bulletin of China* 25: 1295–1298.
- Ju S-B, Wang X-R, Liu Y-C, Wang Y. 2021. A reassessment of *Iteravis huchzermeyeri* and *Gansus zheni* from the Jehol biota in western Liaoning, China. *China Geology* 2: 197–204.
- Lamanna MC, You H-L, Harris JD, Chiappe LM, Ji S-A, Lü J-C, Ji Q. 2006. An enantiornithine (Aves: Ornithothoraces) partial skeleton from the Early Cretaceous of northwestern China. *Acta Palaeontologica Polonica* 51: 423–434.
- LeBlanc AR, Brink KS, Cullen TM, Reisz RR. 2017. Evolutionary implications of tooth attachment versus tooth implantation: A case study using dinosaur, crocodylian, and mammal teeth. *Journal of Vertebrate Paleontology* 37: e1354006.
- Li Y, Zhang Y-G, Zhou Z-H, Li Z-H, Liu D, Wang X-L. 2011. New material of *Gansus* and a discussion on its habit. *Vertebrata Palasiatica* 49: 435–445.
- Li Z-H, Zhou Z-H, Clarke JA. 2018. Convergent evolution of a mobile bony tongue in flighted dinosaurs and pterosaurs. *PLoS ONE* 13: e0198078.
- Linnaeus C. 1758. *Systema naturae per regna tria naturae, secundum classes, ordines, genera, species, cum characteribus, differentiis, synonymis, locis*. Regnum animale. Editio decima, reformata. Stockholm: Laurentii Salvii. 1.
- Liu D, Chiappe LM, Zhang Y-G, Bell A, Meng Q-J, Ji Q, Wang X-R. 2014. An advanced, new long-legged bird from the Early Cretaceous of the Jehol Group (northeastern China): Insights into the temporal divergence of modern birds. *Zootaxa* 3884: 253–266.
- Lü J-C, Brusatte SL. 2015. A large, short-armed, winged dromaeosaurid (Dinosauria: Theropoda) from the Early Cretaceous of China and its implications for feather evolution. *Scientific Reports* 5: 1–11.
- Lü J-C, Kundrát M, Shen C-Z. 2016a. New material of the pterosaur *Gladocephaloideus* Lü et al., 2012 from the Early Cretaceous of Liaoning Province, China, with comments on its systematic position. *PLoS ONE* 11: e0154888.
- Lü J-C, Liu C-Y, Pan L-J, Shen C-Z. 2016b. A new pterodactyloid pterosaur from the Early Cretaceous of the western part of Liaoning Province, northeastern China. *Acta Geologica Sinica-English Edition* 90: 777–782.
- Ma F. 1993. *Late Mesozoic fossil fishes from the Jiuquan Basin of Gansu Province, China*. Beijing: Ocean Press.
- Marsh OC. 1880. *Odontornithes: A monograph on the extinct toothed birds of North America*. Professional Papers of the Engineer Department. U.S. Army 18: 1–201.
- Martin LD, Stewart JD. 1977. Teeth in *Ichthyornis* (Class: Aves). *Science* 195: 1331–1332.
- Martin LD, Stewart JD. 1999. Implantation and replacement of bird teeth. In: Olson SL, Wellnhofer P, Mourer-Chauviré C, Steadman DW, Martin LD eds. *Avian paleontology at the close of the 20th century: proceedings of the 4th International Meeting of the Society of Avian Paleontology and Evolution*, Washington, DC, 4–7 June 1996. 295–300.
- Murray AM, You H-L, Peng C. 2010. A new Cretaceous osteoglossomorph fish from Gansu Province, China. *Journal of Vertebrate Paleontology* 30: 322–332.
- Nudds RL, Atterholt JA, Wang X, You H-L, Dyke GJ. 2013. Locomotory abilities and habitat of the Cretaceous bird *Gansus yumenensis* inferred from limb length proportions. *Journal of Evolutionary Biology* 26: 150–154.
- O'Connor J, Chiappe LM. 2011. A revision of enantiornithine (Aves: Ornithothoraces) skull morphology. *Journal of Systematic Palaeontology* 9: 135–157.
- O'Connor J, Erickson GM, Norell MA, Bailleul AM, Hu H, Zhou Z-H. 2018. Medullary bone in an Early Cretaceous enantiornithine bird and discussion regarding its identification in fossils. *Nature Communications* 9: 1–8.
- O'Connor JK, Chiappe LM, Chuong C-M, Bottjer DJ, You H-L. 2012. Homology and potential cellular and molecular mechanisms for the development of unique feather morphologies in early birds. *Geosciences* 2: 157–177.
- O'Connor JK, Li D-Q, Lamanna M, Wang M, Harris JD, Atterholt JA, You H-L. 2016b. A new Early Cretaceous enantiornithine (Aves: Ornithothoraces) from northwestern China with elaborate tail ornamentation. *Journal of Vertebrate Paleontology* 36: e1054035.
- O'Connor JK, Wang M, Hu H. 2016a. A new ornithuromorph (Aves) with an elongate rostrum from the Jehol biota and the early evolution of rostralization in birds. *Journal of Systematic Palaeontology* 4: 1–10.
- O'Connor JK, Zhou Z-H. 2013. A redescription of *chaoyangia beishanensis* (aves) and a comprehensive phylogeny of mesozoic birds. *Journal of Systematic Palaeontology* 11: 889–906.
- Pérez-Moreno B, Sanz JL, Buscalioni AD, Moratalla JJ, Ortega F, Rasskin-Gutman D. 1994. A unique multitoothed ornithomimosaur dinosaur from the lower Cretaceous of Spain. *Nature* 370: 363–367.
- Shao S, Li L, Yang Y, Zhou C-F. 2018. Hyperphalangy in a new sinemydid turtle from the Early Cretaceous Jehol biota. *PeerJournal* 6: 1–21.
- Suarez MB, Ludvigson GA, Gonzalez LA, Al-Suwaidi AH, You H-L eds. 2013. *Stable isotope chemostratigraphy in lacustrine strata of the*

- Xiagou Formation, Gansu Province, NW China. London: Geological Society.
- Suarez MB, Ludvigson GA, González LA, You H-L. 2017. Continental paleotemperatures from an Early Cretaceous dolomitic lake, Gansu Province, China. *Journal of Sedimentary Research* 87: 486–499.
- Wang M, Li D-Q, O'Connor JK, Zhou Z-H, You H-L. 2015a. Second species of enantiornithine bird from the lower Cretaceous Changma Basin, northwestern China with implications for the taxonomic diversity of the Changma avifauna. *Cretaceous Research* 55: 56–65.
- Wang M, Li Z-H, Liu Q-G, Zhou Z-H. 2020b. Two new Early Cretaceous ornithuromorph birds provide insights into the taxonomy and divergence of Yanornithidae (Aves: Ornithothoraces). *Journal of Systematic Palaeontology* 18: 1805–1827.
- Wang M, O'Connor JK, Bailleul AM, Li Z-H. 2020a. Evolution and distribution of medullary bone: Evidence from a new Early Cretaceous enantiornithine bird. *National Science Review* 7: 1068–1078.
- Wang M, O'Connor JK, Zhou S, Zhou Z-H. 2019. New toothed Early Cretaceous ornithuromorph bird reveals intraclade diversity in pattern of tooth loss. *Journal of Systematic Palaeontology* 18: 1–15.
- Wang M, Stidham TA, Zhou Z-H. 2018a. A new clade of basal Early Cretaceous pygostylian birds and developmental plasticity of the avian shoulder girdle. *Proceedings of the National Academy of Sciences USA* 115: 10708–10713.
- Wang M, Zhou Z-H. 2018. A new confuciusornithid (Aves: Pygostylia) from the Early Cretaceous increases the morphological disparity of the Confuciusornithidae. *Zoological Journal of the Linnean Society* 185: 417–430.
- Wang M, Zhou Z-H. 2020. Anatomy of a new specimen of *Piscivorenantiornis inusitatus* (Aves: Enantiornithes) from the lower Cretaceous Jehol biota. *Journal of Vertebrate Paleontology* 40: e1783278.
- Wang M, Zhou Z-H, Sullivan C. 2016a. A fish-eating enantiornithine bird from the Early Cretaceous of China provides evidence of modern avian digestive features. *Current Biology* 26: 1170–1176.
- Wang M, Zhou Z-H, Zhou S. 2016b. A new basal ornithuromorph bird (Aves: Ornithothoraces) from the Early Cretaceous of China with implication for morphology of early Ornithuromorpha. *Zoological Journal of the Linnean Society* 176: 207–223.
- Wang R-F, Wang Y, Hu D-Y. 2015b. Discovery of a new ornithuromorph genus, *Juehuaornis* gen. nov. from lower Cretaceous of western Liaoning, China. *Global Geology* 34: 7–11.
- Wang S, Stiegler J, Wu P, Chuong C-M, Hu D-Y, Balanoff A, Zhou Y-C, Xu X. 2017a. Heterochronic truncation of odontogenesis in theropod dinosaurs provides insight into the macroevolution of avian beaks. *Proceedings of the National Academy of Sciences USA* 114: 10930–10935.
- Wang X, Huang J-D, Hu Y-C, Liu X-Y, Peteya JA, Clarke JA. 2018b. The earliest evidence for a supraorbital salt gland in dinosaurs in new Early Cretaceous ornithurines. *Scientific Reports* 8: 1–12.
- Wang X, Zhou Z. 2003. Mesozoic pompeii. In: Chang M, Chen P, Wang Y, Wang Y, Miao D eds. *The Jehol biota: the emergence of feathered dinosaurs, beaked birds and flowering plant*. Shanghai: Shanghai Scientific and Technical Publishers. 19–35.
- Wang X-L, Rodrigues T, Jiang S-X, Cheng X, Kellner AWA. 2014. An Early Cretaceous pterosaur with an unusual mandibular crest from China and a potential novel feeding strategy. *Scientific Reports* 4: 1–9.
- Wang Y, Hu H, O'Connor JK, Wang M, Xu X, Zhou Z-H, Wang X-L, Zheng X-T. 2017b. A previously undescribed specimen reveals new information on the dentition of *Sapeornis chaoyangensis*. *Cretaceous Research* 74: 1–10.
- Wang Y-M, O'Connor JK, Li D-Q, You H-L. 2013. Previously unrecognized ornithuromorph bird diversity in the Early Cretaceous Changma Basin, Gansu Province, northwestern China. *PLoS ONE* 8: e77693.
- Wang Y-M, O'Connor JK, Li D-Q, You H-L. 2016c. New information on postcranial skeleton of the Early Cretaceous *Gansus yumenensis* (Aves: Ornithuromorpha). *Historical Biology* 28: 666–679.
- You H, O'Connor J, Chiappe LM, Ji Q. 2005. A new fossil bird from the Early Cretaceous of Gansu Province, northwestern China. *Historical Biology* 17: 7–14.
- You H-L, Atterholt JA, O'Connor JK, Harris JD, Lamanna MC, Li D-Q. 2010. A second ornithuromorph from the Changma Basin, Gansu Province, northwestern China. *Acta Palaeontologica Polonica* 55: 617–625.
- You H-L, Lamanna MC, Harris JD, Chiappe LM, O'Connor J, Ji S-A, Lü J-C, Yuan C-X, Li D-Q, Zhang X, Lacovara KJ, Dodson P, Ji Q. 2006. A nearly modern amphibious bird from the Early Cretaceous of northwestern China. *Science* 312: 1640–1643.
- Zhang X-J, Jiang S-X, Cheng X, Wang X-L. 2019. New material of *Sinopterus* (Pterosauria, Tapejaridae) from the Early Cretaceous Jehol biota of China. *Anais de Academia Brasileira de Ciências* 91: e20180756.
- Zhou S, Zhou Z-H, O'Connor JK. 2012. A new toothless ornithurine bird (*Schizooura lii* gen. et sp. nov.) from the lower Cretaceous of China. *Vertebrata Palasiatica* 50: 9–24.
- Zhou S, Zhou Z-H, O'Connor JK. 2013. Anatomy of the Early Cretaceous *Archaeorhynchus spathula*. *Journal of Vertebrate Paleontology* 33: 141–152.
- Zhou S, O'Connor JK, Wang M. 2014. A new species from an ornithuromorph dominated locality of the Jehol Group. *Chinese Science Bulletin* 59: 5366–5378.
- Zhou Z, Clarke J, Zhang F. 2008. Insight into diversity, body size and morphological evolution from the largest Early Cretaceous enantiornithine bird. *Journal of Anatomy* 212: 565–577.
- Zhou Z, Zhang F. 2001. Two new ornithurine birds from the Early Cretaceous of western Liaoning, China. *Chinese Science Bulletin* 46: 1258–1264.
- Zhou Z, Zhang F. 2005. Discovery of an ornithurine bird and its implication for Early Cretaceous avian radiation. *Proceedings of the National Academy of Sciences USA* 102: 18998–19002.

Supplementary Material

The following supplementary material is available online for this article at <http://onlinelibrary.wiley.com/doi/10.1111/jse.12823/supinfo>:

Fig. S1. Early photograph of IVPP V26196 showing the impression in the sediment of the rostrum. Photo by Barbara Marrs.

Fig. S2. Results of the cladistic analysis, first round of tree-bisection reconnection (length = 896 steps; CI = 0.367; RI = 0.654).

Fig. S3. Strict reduced consensus tree (*Chaoyangia* removed) of the 10 000 trees recovered by the second round of tree-bisection reconnection (length = 896 steps).